INVESTIGATION OF INFLUENCE OF DRUGS ON CELLULAR METABOLISM IN 2D CELL CULTURE USING SURFACE-ENHANCED RAMAN SCATTERING

by
Ayşe Çınkılıç

Submitted to Graduate School of Natural and Applied Sciences
in Partial Fulfillment of the Requirements
for the Degree of Master of Science in
Biotechnology

Yeditepe University
2021

INVESTIGATION OF INFLUENCE OF DRUGS ON CELLULAR METABOLISM IN 2D CELL CULTURE USING SURFACE-ENHANCED RAMAN SCATTERING

APPROVED BY:

Prof. Dr. Mustafa Çulha ……
(Thesis Supervisor)
(University of South Florida)

Assist. Prof. Dr. Gülengül Duman ……
(Yeditepe University)

Assoc. Prof. Kaan Keçeci ……
(Medeniyet University)

DATE OF APPROVAL: ..../..../2021

I hereby declare that this thesis is my own work and that all information in this thesis has been obtained and presented in accordance with academic rules and ethical conduct. I have fully cited and referenced all material and results as required by these rules and conduct, and this thesis study does not contain any plagiarism. If any material used in the thesis requires copyright, the necessary permissions have been obtained. No material from this thesis has been used for the award of another degree.

I accept all kinds of legal liability that may arise in case contrary to these situations.

Name, Last name Ayşe Çınkılıç.....……

Signature …..…….……..

Dedicated to my MOM …

ACKNOWLEDGEMENTS

I would like to thank my supervisor Prof. Dr. Mustafa Çulha who give me opportunity to study in his laboratory and encourage me with his great suggestions and comments during my thesis period. Pursuing my thesis under his supervision has been an experience which broadens the mind and presents an unlimited source of learning.

I would like to thank Deniz Yılmaz, Hande Duru, Dr. Mine Altunbek and Zehra Çobandede, for being my friends, so supportive, for helpful and motivated; I wouldn't have finished this thesis without them, they always insist me to writing my thesis and help during to experimental parts. I would like to thank Dr. Hülya Yılmaz for her help in developing this thesis design. I also would like to thank Dr. Melike Sarıçam, Dr. Cansu Ümran Tunç, Dr. Pınar Akkuş, Dr. Şaban Kalay, Dr. İnci Kurt Celep, İpek Bedir, Selen Tiryaki, Ece Nazır.

I also would like to thank my dearest friend Seçil Durel, she always supported me when I cried or depressive she always gives me hope and happiness. I’m happy to you are my best friend.

I especially thank you for Orçun Bayrak, he always supported me, he was with me in every difficulty, and he searched articles for me even though he had no knowledge about it. I’m grateful for him patience through in my thesis writing period.

My parents and my brothers they always supported me in terms of everything in my thesis and also in my life. I’m so grateful for their encouragement and motivation. I’m lucky to have them.

ABSTRACT

INVESTIGATION OF INFLUENCE OF DRUGS ON CELLULAR METABOLISM IN 2D CELL CULTURE USING SURFACE-ENHANCED RAMAN SCATTERING

Raman spectroscopy (RS) is a powerful vibrational spectroscopic technique that provides molecular-level information from a sample without a label. Surface-enhanced Raman scattering (SERS) is a highly sensitive mode of Raman Spectroscopy and it can help to identify molecular composition on the surface or very close vicinity of noble metal particles with a size of fewer than two orders of magnitude in seconds. Metformin (MET) is a drug molecule, which affect mitochondrial respiratory chain complex I, cell proliferation, protein synthesis and gluconeogenesis. 6-Mercaptopurine (6-MP) has immunosuppressive features that conceivable regulated by its involvement with nucleic acid metabolism and protein synthesis in the series following antigen stimulation, and via its cytotoxic activity on cells. In this study, the potential of SERS to be able to monitor the effect of drugs on cell metabolism was investigated using metformin and 6-Mercaptopurine as model drugs. Two cell lines, A549 and Beas-2b, were chosen for the study. Gold nanoparticles with an average size of 50 nm were chosen as SERS substrates. Nucleic acids, amino acids and phospholipids peaks were changed in treatment of Metformin. The reason for this change MET mechanisms which inhibition of proliferation and protein synthesis and suppression of lipid and cholesterol biosynthesis. SERS peaks corresponding to nucleic acids and proteins were changed with the treatment of 6-Mercaptopurine. The observed spectral changes are attributed to the inhibition of de novo purine synthesis and protein synthesis. The changes in observed spectral pattern upon exposure of cells to drug molecules at increasing concentrations are attempted to relate the known drug metabolism mechanisms. The results demonstrate that SERS can be used to monitor the metabolic changes at cellular level upon exposing them to drug molecules as it is demonstrated in the case of MET and 6-MP.

ÖZET

YÜZEYDE ZENGİNLEŞTİRİLMİŞ RAMAN SAÇILIMI KULLANILARAK 2D HÜCRE KÜLTÜRÜNDE İLAÇLARIN HÜCRESEL METABOLİZMA ÜZERİNDEKİ ETKİSİNİN İNCELENMESİ

Raman spektroskopisi (RS), etiketsiz bir numuneden moleküler düzeyde bilgi sağlayan güçlü bir titreşim spektroskopik tekniktir. yüzeyde zenginliştirilmiş Raman saçılımı (SERS), Raman Spektroskopisinin oldukça hassas bir modudur ve yüzeydeki moleküler bileşimi veya çok yakın çevresindeki soy metal partiküllerin boyutu, saniyede iki büyüklükten daha az büyüklükte tanımlanmasına yardımcı olabilir. Metformin (MET), mitokondriyal solunum zinciri kompleksi I, hücre proliferasyonu, protein sentezi ve glukoneogenezi etkileyen bir ilaç molekülüdür. 6-Merkaptopürin (6-MP), antijen uyarımını takiben serideki nükleik asit metabolizması ve protein senteziyle ilgisi ve hücreler üzerindeki sitotoksik aktivitesi ile düzenlenebilen immünosüpresif özelliklere sahiptir. Bu çalışmada, SERS'in ilaçların hücre metabolizması üzerindeki etkisini izleyebilme potansiyeli, model ilaçlar olarak metformin ve 6-Merkaptopurin kullanılarak araştırılmıştır. Çalışma için iki hücre hattı, A549 ve Beas-2b seçildi. Ortalama boyutu 50 nm olan altın nanopartiküller, SERS substratları olarak seçildi. Metformin tedavisinde nükleik asitler, amino asitler ve fosfolipid zirveleri değişti. Bu değişikliğin nedeni, proliferasyonun inhibisyonunu ve protein sentezini ve lipid ve kolesterol biyosentezinin baskılanmasını sağlayan MET mekanizmalarıdır. Nükleik asitlere ve proteinlere karşılık gelen SERS pikleri, 6-Merkaptopürin tedavisi ile değiştirildi. Gözlemlenen spektral değişiklikler, de novo purin sentezinin ve protein sentezinin engellenmesine atfedilir. Hücrelerin artan konsantrasyonlarda ilaç moleküllerine maruz kalması üzerine gözlemlenen spektral modeldeki değişiklikler, bilinen ilaç metabolizması mekanizmalarıyla ilişkilendirilmeye çalışılır. Sonuçlar, MET ve 6-MP durumunda gösterildiği gibi, SERS'in ilaç moleküllerine maruz kalması üzerine hücresel düzeyde metabolik değişiklikleri izlemek için kullanılabileceğini göstermektedir.

TABLE OF CONTENTS

ACKNOWLEDGEMENTS v

ABSTRACT vi

ÖZET vii

LIST OF FIGURES x

LIST OF SYMBOLS/ABBREVIATIONS xii

1. INTRODUCTION 1

1.1. RAMAN SPECTROSCOPY 1

1.2. RAMAN SPECTROSCOPY IN LIVING CELL ANALYSIS 2

1.3. RAMAN SPECTROSCOPY IN DRUG-CELL STUDIES 3

1.4. SERS 4

1.5. SERS SINGLE CELL 5

1.6. SERS CELLULAR DRUG STUDIES 6

1.7. METFORMIN 7

1.7.1. Brief History of Metformin 7

1.7.2. Metformin and Diabetes 8

1.7.3. Cellular Uptake of Metformin 8

1.7.4. Mechanism of Metformin 9

1.7.5. AMPK- Dependent and –Independent Mechanisms 10

1.7.6. Inhibition of Gluconeogenesis 11

1.7.7. Regulation of Lipid Metabolisms 12

1.7.8. Metformin Prevents Cell Death 12

1.7.9. Metformin Action of Cancer 13

1.7.10. Metformin Effect on Endocytic Cycle 14

1.8. 6-MERCAPTOPURINE 15

1.8.1. History of 6-Mercaptopurine 15
1.8.2. Mechanism of 6-Mercaptopurine 16
1.8.3. Thiopurine Methyltransferase Enzyme (TPMT) 20
1.8.4. *De Novo* Purine Synthesis Inhibitions of 6-Mercaptopurine 21
1.8.5. Anticancer Effect of 6-Mercaptopurine 22
2. MATERIALS 23
2.1. CHEMICALS AND REAGENTS 23
2.2. INSTRUMENTS 23
2.3. CELL LINES 23
3. METHODS 24
3.1. GOLD NANOPARTICLES SYNTHESIS 24
3.2. GOLD NANOPARTICLES CHARACTERIZATIONS 24
3.3. CELL CULTURE 24
3.4. WST-1 CELL PROLIFERATION ASSAY 24
3.5. SERS MEASUREMENTS 25
3.6. STATISTICAL ANALYSIS 26
4. RESULTS AND DISCUSSION 27
4.1. CHARACTERIZATION OF GOLD NANOPARTICLES 27
4.1.1. UV/Vis Spectroscopy 27
4.1.2. Dynamic Light Scattering 27
4.2. WST-1 CELL PROLIFERATION ASSAY 28
4.3. SERS MEASUREMENT 30
5. CONCLUSION AND FUTURE PERSPECTIVES 41
REFERENCES 44

LIST OF FIGURES

Figure 1.1. Demonstration of (a) Raman and Rayleigh scattering (green: no energy difference (v0 depicts laser frequency), red: incident photon loss energy (Stokes scattering), blue: incident photon gain energy (and anti-Stokes scattering)), (b) graphical representation ..... ….2

Figure 1.2. Difference between the Raman and the SERS technique..... 4

Figure 1.3. Chemical structure of MET 7

Figure 1.4. Molecular mechanism of MET..... 10

Figure 1.5. Energy metabolism regulation by AMPK.. 11

Figure 1.6. Molecular structure of 6-MP 16

Figure 1.7. Schematic representation of 6-MP mechanisms 18

Figure 1.8. Polymorphisms in the 6-MP intracellular pathway have been related to an adverse effects increased risk 21

Figure 4.3.1. Average SERS spectra of Beas-2b cell line at increasing MET concentrations ……..32

Figure 4.3.2. Comparison of (a) first and (b) second PCs of control and MET treated Beas-2b cells 33

Figure 4.3.3. SERS spectra of A549 cell line at increasing MET concentrations 35

Figure 4.3.4. Comparison of (a) first and (b) second PCs of control and MET treated A549 cells 36

Figure 4.3.5. Average SERS spectra of Beas-2b cell line at increasing 6-MP concentrations ……..37

Figure 4.3.6. Comparison of (a) first and (b) second PCs of control and 6-MP treated Beas cells 37

Figure 4.3.7. SERS spectra of A549 cell line at increasing 6-MP concentrations 39

Figure 4.3.8. Comparison of (a) first and (b) second PCs of control and 6-MP treated A549cells 40

LIST OF SYMBOLS/ABBREVIATIONS

AgNPs	Silver nanoparticles
AuNPs	Gold nanoparticles
CuO	Copper (II) oxide
CV	Coefficient of variation
DLS	Dynamic light scattering
DNA	Deoxyribonucleic acid
ELISA	Enzyme-linked immunosorbent assay plate reader
Fe_3O_4	Iron (II,III) oxide
$HAuCl_4$	Hydrogen tetrachloroaurate
LDA	Linear discriminant analysis
nm	Nanometer
nM	Nanomolar
NPs	Nanoparticles
NMR	Nuclear magnetic resonance
PBS	Phosphate-buffered saline
PCA	Principle component analysis
PDMS	Polydimethylsiloxane
Phe	Phenylalanine

1. INTRODUCTION

1.1. RAMAN SPECTROSCOPY

Raman Spectroscopy (RS) is a powerful vibrational and analytical technique, which provides molecular level information from a sample without a label. RS is explored by Chandrasekhara Venkata Raman in 1928 [1].

RS mechanism is based on the Raman Scattering effect. As molecule's electric dipole interacts with an incident photon, scattering happens. This mechanism may be elastic or inelastic. Rayleigh scattering is a form of incident photon scattering in which photons are scattered elastically by a molecule. Incident photons energy is equals with scattered photons energy, in Rayleigh scattering. Small fraction of light is Raman scattering which is scattered at energies different than that of the incident photons (Raman Effect). Two kinds of Raman scattering; 1) Stokes scattering-phonon emitted which means scattered photons have a lower energy, 2) anti-Stokes scattering-phonon absorbed which means scattered photons have a higher energy. Figure 1.1. shows Rayleigh and Raman scattering. Figure 1.1.(a). shows a simplified energy diagram that illustrates these terms. Even at low vibrational energy, the Stokes and anti-Stokes Raman peaks are symmetrically located around the Rayleigh peak, but their intensities are quite different [2]. Figure 1.1.(b). illustrates a model Raman spectrum. Since most molecules that in the lowest vibrational energy state at room temperature, anti-Stokes Raman peaks have much lower intensities than Stokes Raman peaks [2].

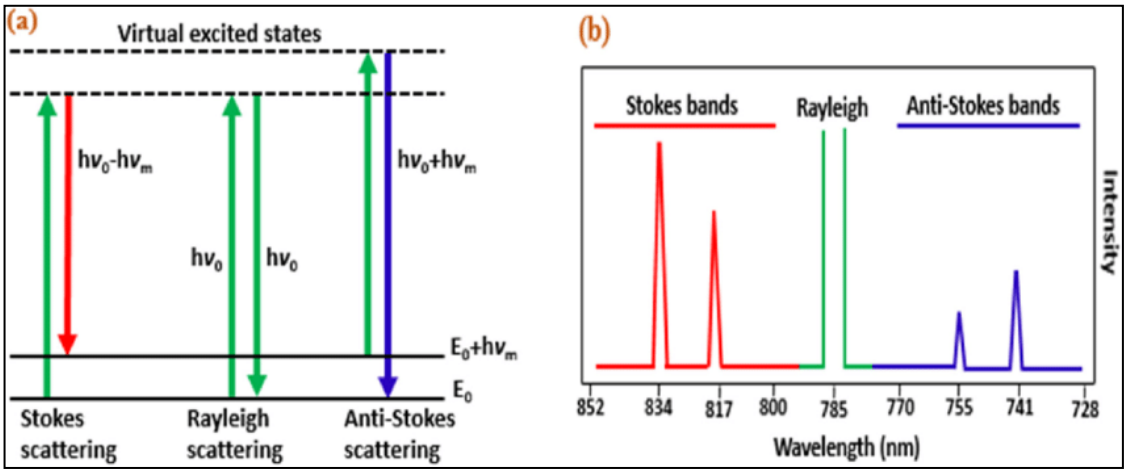

Figure 1.1. Demonstration of (a) Raman and Rayleigh scattering (green: no energy difference (v0 depicts laser frequency), red: incident photon loss energy (Stokes scattering), blue: incident photon gain energy (and anti-Stokes scattering)), (b) graphical representation [2]

Raman spectroscopy has some advantages with label-free, rapid analysis, less sensitivity to water, and non-destructive nature over FTIR spectroscopy, another vibrational spectroscopic technique, as commonly compared. The Raman spectrum provides rich information to chemical structure of biological samples that makes RS technique quite promising tool in biological applications.

1.2. RAMAN SPECTROSCOPY IN LIVING CELL ANALYSIS

In tissue and also a single cell, the Raman spectrum ensures details about chemical bonds related with biomolecules such as proteins, lipids, DNA, and RNA. Structure, composition, conformation, identity and macromolecules interactions (such as protein-DNA) can be provided by RS for biological samples. Cells can be analyzed in aqueous conditions, water shows weak Raman signal, therefore analysis of living cells can observation by Raman spectroscopy under their physiological environments such as cell medium or phosphate buffer solution (PBS) [3]. Thus, RS used for single-cell analysis, cancer diagnosis also drug delivery in living cells. In one of the earliest studies, the cell was fixed with alcohols or aldehydes for RS analysis as in traditional cell analysis. Then, using fixed cells; cells

organelles were observed which are nucleic acids [4], proteins [5], lipids [6], mitochondria [7] and even stage of the cell cycle [8]. However, other studies show that fixed cells are not correct method to cell analyzed because they can give incorrect Raman spectra and this data being misinterpreted [9–12]. For this reason, cells can use without any fixation method for RS sample.

One of the studies about single cell in PBS and without fixation is observed on human erythrocytes for oxygenation process. According to measured intensity changing cell deoxygenation were detected before the reoxygenated process as a time-dependently. This study result illustrates RS can use for this process to followed and demonstrated [13]. Also RS can use for cancer cells analysis such as ovarian, prostate and breast cancer cells [14–18] Also, the cell cycle can analysis with Raman spectroscopy. Swain et al are investigated cell cycle phases on osteosarcoma cells by RS. Cell cycle phases which are G0–G1, S, and G2–M were illustrated according to changing Raman spectra on a living single cell [19]. Further, different cells can be determined with RS. In an early study, different type of bone cells was discriminate against by RS [20]. In another study, RS used for determine different type of cancer cells which are human breast and human leukemia cells, and MCF-7 human cancer and human sarcoma cells, based on their spectra [21].

1.3. RAMAN SPECTROSCOPY IN DRUG-CELL STUDIES

Raman spectroscopy also used for evaluation of the effects of the small molecules as pharmaceutical applications. Drug cell interaction can investigate with RS that examination of presence of drug and drug effects in cell. RS provide long-term drug effects monitoring in the cell or minimal dose determination of drug [22]. One of the studies about drug research by RS is that different concentration of chemotherapeutic drug, cisplatin, effect on lung adenocarcinoma cells to 96 h [23]. Another use of the RS for drugs studies is that investigate noncytotoxic dose determination. A related study that investigates gemcitabine, anticancer drug, noncytotoxic effects and the study showed DNA and protein changes according to time and doses in single living cells [24]. Apoptotic effects of fluorouracil were investigated which drug-induced results related to lipids, nucleic acids and proteins bands decreasing intensity on gastric carcinoma cells [25]. Moreover, active pharmaceutical ingredient (API) characterization and drug-excipient interaction can determine with RS and also critical

quality attributes of pharmaceutical products (CQAs) can evaluate [26,27] Drugs can be visualized intracellularly in the way of label-free method. The related study is that the entry of the paclitaxel which is an anticancer drug into the cytoplasm through the cell membrane was observed by measuring RS in breast cells [28]. Using RS, mechanisms and action of Doxorubicin were analyzed on cancer cells which are A549 and Calu-1. The drugs show the different effect of two different cell lines according to Raman spectra and also results correlated with drugs mechanisms which change bcl-2 protein expression and reactive oxygen species (ROS) levels [29]. Further, cellular uptake binding and cellular responses of drugs can elucidate with Raman spectroscopy. One of the studies that investigated Doxorubicin, Actinomycin, Cisplatin and Vincristine drugs on lung cancer cell lines. The results illustrated different anticancer drugs have different action, pathways and also different Raman spectra depending on their dose in a label-free manner [30].

1.4. SERS

Fleischman and his colleague first investigated Raman signal of pyridine on the silver electrode [31]. Then, the first experiment for strong Raman signaling achieved on pyridine molecules was measured on a rough silver electrode that provides 10^5-10^6 Raman scattering enhancement, R. Van Duyne and D. Jeanmarie in 1997 [32]. After that time SERS-active substrates were approved on various molecules that have strong enhancement Raman signals [33]. SERS-active substrates can be different shape, size and nanomaterials. Generally, silver and gold nanoparticles use as a SERS-active substrates and the size range is between 10-150 nm [34].

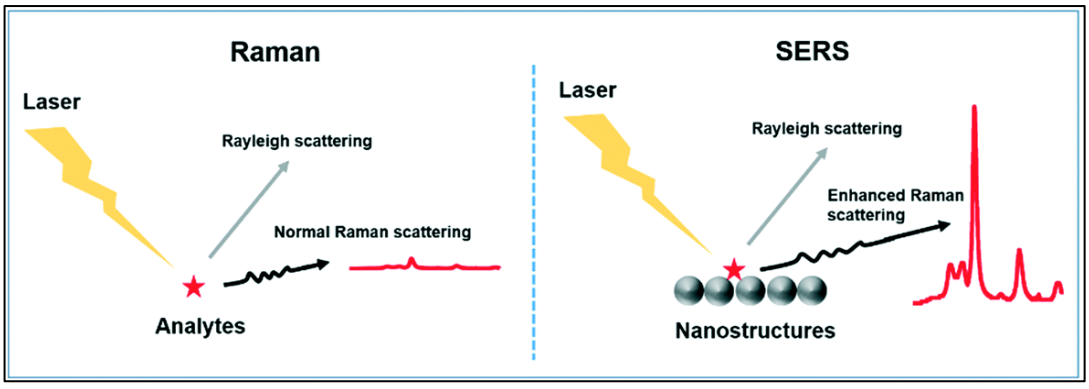

Figure 1.2. Difference between the Raman and the SERS technique [35]

SERS enhancement mechanisms explained as two mechanisms which are chemical (CE) and electromagnetic (EM) enhancement [36]. In 1977, Albrecht and Creighton explained chemical enhancement. The reason for occurrence of chemical enhancement is that molecular polarizability increasing which owing to sample molecule and metal charge transfer and specific interactions, forming charge-transfer complexes. The surface absorbs molecules then metal and molecules, electronic states can interact with each other herewith new transitions were produced, which leads to Raman signal enhancement. Chemical enhancement magnitude is ~10-100 times. An electromagnetic enhancement mechanism was offered by Van Duyne and Jeanmarie. On the metal surface, incident electric field (from incident radiation) interact with electron, thus electromagnetic enhancement has occurred. Hereby, this leads to electric field enhancement and surface plasmons excitation at the metal surface [37].

1.5. SERS SINGLE CELL

In 1991, Nabiev et al. have reported SERS single-cell analysis as the first study [38]. The study achieved with antitumor drugs which are doxorubicin (DOX), and 4'O-tetrahydropyranyl-adriamycin (THP-ADM) were treated with erythroleukemic K562 cells also AgNPs were used for SERS substrates. The results show SERS signals come from living single-cell nucleus or cytoplasm when treated with much diluted drugs. These results bring to light SERS is a new technique for cancer research and single-cell studies. Afterwards, Kneipp et al. proposed a second single living cell measurement with SERS using 60 nm AuNPs, in 2002 [39]. They observed intracellular fragments such as DNA and phenylalanine on differentiated intestinal epithelial cells HT29 from SERS signals. Results of study illustrate SERS ensure selective and sensitive analysis of living single cell.

Various single-cell SERS studies with AuNPs has been working for many years [40]. Some of studies focused on determining intracellular organic compound of single-cell using gold colloids in 2005 [41], gold nanorods which are anti-EGFR conjugated used for human oral cancer diagnostic marker in 2007 [42], in human cells using gold nanoparticles effective intracellular quantification of dinitrophenol derivative (DAMP) were showed in 2008 [43], gold nanoparticles transportation on the cell surface also into the cell were observed, 2009 [44].

In recent years SERS has various applications range such as chemistry, physics, nanoscience and biological science [45–48] It is well known SERS studies increase about in biological area. Further, it was provided with an opportunity to finding novel applications such as SERS-based label-free probing DNA hybridization [49] and in vivo tumor targeting [50]. SERS studies can occur in a label-free manner which is SERS spectra of biomolecules measure without any Raman dyes. For detecting biomolecules SERS-based label-free detection ensures a highly sensitive, selective direct and reliable method and also it is convenient rather than the SERS labeling method [51]. According to Hong-Wu Tang et al. study, chemical information of human osteosarcoma cells was investigated in detailed in both living or fixed single cells using 60 nm colloidal gold nanoparticles [52]. Thus, they show SERS is a powerful technique in biomedicine studies. In recent work, single-cell cellular responses were evaluated with SERS based nuclear-targeted AuNPs. In this study, modifications were observed on lipid and protein structures due to nuclear-targeted AuNPs thus cause plasmonic photothermal therapy (PTT) cell death [53].

1.6. SERS CELLULAR DRUG STUDIES

Quantitative and qualitative information about the various structure is achieved by SERS even pharmaceutical analysis. Most pharmaceutical molecules demonstrate good Raman spectra including diluted concentrations. SERS provide to cost and time-saving for pharmaceutical analysis because of its direct and easy usage [37].

SERS can use for drug monitoring as quantitative analysis. One of the studies about drug monitoring is that anti EGFR small molecule is erlotinip using for non-small cell lung and pancreatic cancer treatment. The nanomolar drug concentration was detected by SERS using gold nanostructure in human plasma samples [54].

Another quantitative SERS drug study was reported by Han et al. [55]. This study investigated 6-Mercaptopurine (6-MP) metabolism in a living cell using Au@Ag NPs for SERS signaling. Firstly, drug uptake into the cell, 6-MP and its metabolic product 6-mercaptopurine-ribose were determined with SERS according to time. The result shows that SERS is efficient and simple for drug efficacy and determine the antitumor drug molecular mechanism in the cell. A similar study about SERS drug study is achieved on 6-MP and methimazole in living Hela cells using AgNPs [56]. The drugs were metabolized and

diffused in the intracellular matrix. Also, metabolism speed was different two drugs that 6-MP faster than methimazole. The results show SERS can applied drug metabolism as a quantitative study in living cell.

1.7. METFORMIN

1.7.1. Brief History of Metformin

The history of the MET (N',N'-dimethylbiguanide), phenformin and buformin began with the *Galega officinalis,* which is also known French lilac*,* extracts that name is galegine which is isoprenyl derivative. It was developed for hyperglycemia type2 diabetes treatments [57]. This extract has include rich guanidine molecules and it was used for the treatment of halitosis and Polyuria in Chinese medicine and middle ages Europe [59,60]. It was reported that hypoglycemic properties of guanidine have too toxic properties for clinical usage in 1918. On the other hand, in vivo studies shows MET include dimethyl biguanide has powerful effects on the arrangement of blood glucose levels, at same time [60]. But, in the same period, for diabetes treatments of MET clinical applications was encumbered because insulin was discovered. Furthermore, buformin and phenformin which are efficacious biguanide derivatives was used for T2DM treatment [61]. MET for clinical growth, also known as Glucophage (glucose eater), is the best antidiabetic agent alternative. It was researched by physician Jean Sterne and Aron Laboratories in the 1950s [62]. MET was accepted to use in the United States, 1995, the United Kingdom, 1958, and Canada, 1972. In 2009, for the Study of Diabetes recommended MET as the first-line oral treatment to T2DM [63]. Additionally, MET is use for polycystic ovary syndrome treatment and also anticancer and antiviral properties of MET being explored.

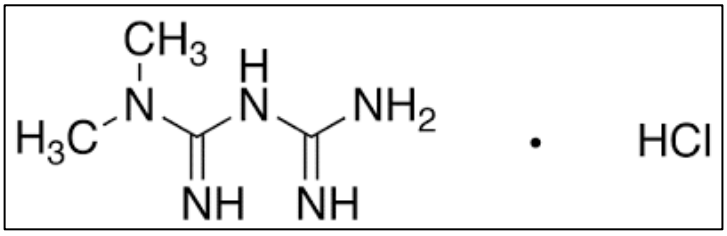

Figure 1.3. Chemical structure of MET

1.7.2. Metformin and Diabetes

382 million people suffer from diabetes according to global data [64]. In 2035, this number is forecast to expand by 592 million presenting national healthcare systems. Factors that cause this are sedentary behavior, rising obesity and increasing urbanization. Also, impaired insulin secretion or insulin resistance related hyperglycaemia results from characterizes T2D. The use of antihyperglycaemic agents, metformin, can be a delay or prevent the beginning of that complications via blood glucose levels management. Although MET was originally introduced for the treatment of T2D, the mechanism of MET is not completely understood. In peripheral tissues, elevated uptake of glucose and increased hepatic insulin sensitivity are related to the anti-hyperglycemic effect of MET. Further, hepatic gluconeogenesis suppression cause metformin acts predominantly which is now commonly admitted. Diabetic patients gluconeogenesis rate can cause to fall approximately 36 percent by use of MET [65]. However, reduction in glucose production pathways still a matter of debate. Bioguanides have antihyperglycemic action which is substantially liver gluconeogenesis inhibition result of reduced glucose and in the skeletal muscle insulin-mediated glucose uptake is increased, probably as smaller rate [67,68].

1.7.3. Cellular Uptake of Metformin

One of the unusually hydrophilic drugs is MET. Under physiological conditions MET charge form generally positively protonated. Rapid and passive diffusion to the cell membranes is not possible because of the physicochemical properties of MET. Organic transporters which have solute carrier property provide active uptake for MET transportation through cell membranes. Also MET enter and leaves cells via multidrug also toxin extrusion (MATE) transporters [67] Plasma membrane monoamine transporter (PMAT, SLC29A4 gene) at on the enterocytes luminal side, mediated MET intestinal absorption as a primarily. Organic cation transporter 1 (Oct1, SLC22A1 gene) is may be in charge of the MET transportation into interstitial fluid and it is expressed on the basolateral membrane of enterocytes [68]. Basolateral membrane of hepatocytes provides OCT3 (SLC22A3 gene) expression. OCT1 and OCT3 are main mediators of hepatic metformin uptake. In liver or biliary excretion, MET does not undergo related biotransformation because renal elimination effect metformin clearance. OCT2 (SLC22A2 gene) provide MET to be carried inside renal epithelial cells,

on the basolateral membrane expression is occurred, urine has include excreted which by multidrug and toxin extrusion 1 and 2 (MATE1 gene SLC47A1 and MATE2 gene SLC47A2) [69].

1.7.4. Mechanism of Metformin

When MET enter the hepatocyte, it accumulates in mitochondrial matrix. Membrane potential of energized mitochondria effects the positively-charged molecule which is consequences of MET uptake [70]. Between the mitochondrial membrane, hydrophobic phospholipids and apolar hydrocarbon side chain of MET may interact [71]. MET main target is that the mitochondrial respiratory chain complex I. MET only inhibits complex I substrates oxidation, its not effects substrates of complex II or IV [70,72]. Despite the fact that these observations were derived from rat hepatocytes on the other hand human hepatocytes and various cell models findings are similar to obtained results [73]. Due to MET has metal-binding features, the drug can inhibits complex I, but it is not clear. Mitochondrial matrix pH raised high. MET is transformed by high mithochondrial matrix ph into a deprotonated structure with high affinity for copper ions [74]. That copper complexes can interfere with respiratory chain sensitive redox reactions. Hereby, MET cellular effects are linked to its capacity of bind copper [75]. Bridges et al. find as an alternative mechanism of complex I inhibition due to MET effects. According to Bridges et al., Ubiquinone reduction inhibits MET in a non-competitive way, likely through binding at interaction of the hydrophilic and membrane domains also keeping the enzyme in deactivated state similar to an open-loop. MET inhibitory effect usually limited to complex I, on the other hand other biaguanides are non-specific that inhibit various mechanisms [76,77]. When ADP and AMP levels increase, ATP production is decreased due to inhibiton of complex I by MET. The cells primary energy sensor, AMP activated protein kinase (AMPK), senses cellular energy charge. MET action shown AMPK-dependent and -independent mennar.

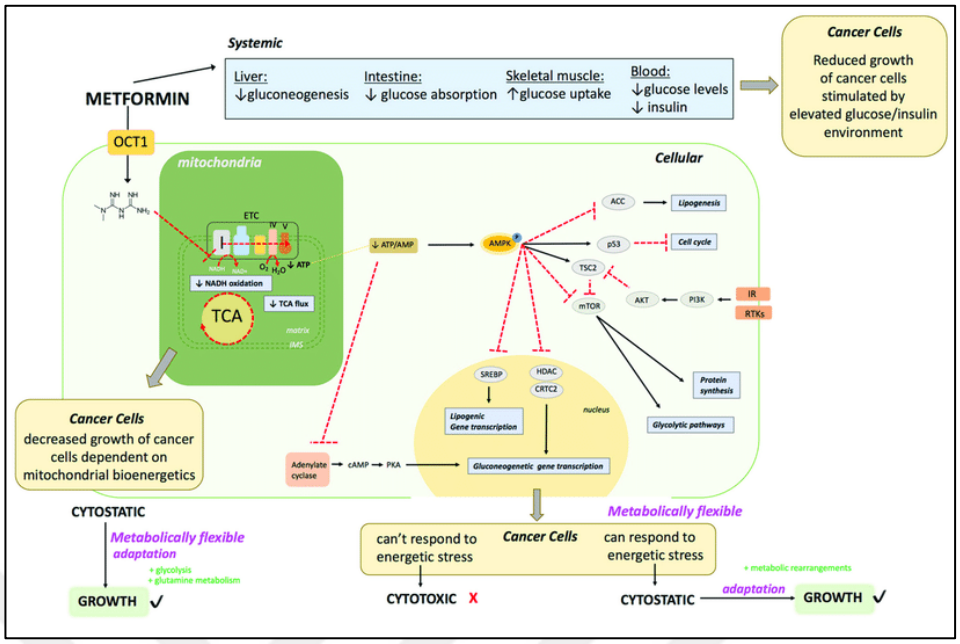

Figure 1.4. Molecular mechanism of MET[78]

1.7.5. AMPK- Dependent and –Independent Mechanisms

Cellular energy homoeostasis regulator is AMPK that activated via AMP or ADP molecules [79]. It provides to the energy status falling to cell respond via converting it from ATP consuming anabolic status to ATP-producing catabolic status. Zhou et al. demonstrated the AMPK role on MET mechanisms in 2001 [80]. According to Zhou et al. in rat primary hepatocytes AMPK activation is stimulated by MET. For the inhibitory effect of MET, AMPK is necessary on glucose production, used the AMPK inhibitor compound C [80]. But the latest research shows that this inhibitor is non-selective. Although, Shaw et al. were supported these findings [81], which found hepatic liver kinase B1 (LKB1) loss, phosphorylating is carried out by catalytic α-subunit of AMPK upstream activator, glucose-lowering effects of MET removed in mice with high-fat diet. Since cAMP response element-binding protein (CREB)-regulated transcription coactivator 2 (CRTC2) is located in nucleus, MET activates the LKB1/AMPK pathway, which alters the cell's gluconeogenic programmed, a pivotal regulator of gluconeogenic gene expression [81]. In Figure 1.5. Represent to AMPK metabolism. Glycogen and gluconeogenesis, as well as fatty acid and cholesterol production, are both inhibited when AMPK is enabled. Glycolysis, glucose uptake also fatty acid oxidation are all activated by AMPK.

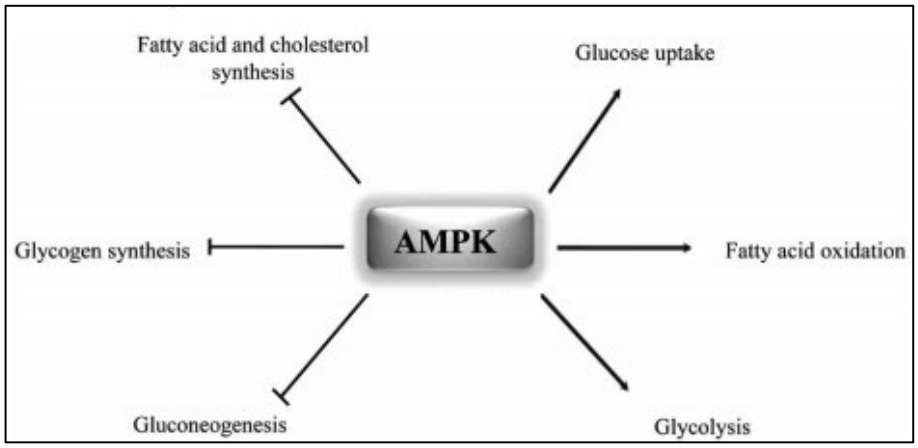

Figure 1.5. Energy metabolism regulation by AMPK [82]

1.7.6. Inhibition of Gluconeogenesis

MET considered as the main site of action in liver that expresses SLC22A1 as a high level. MET can show accumulation in the liver because in the portal circulation it illustrates higher concentration more than another place in the body. Glycogen synthesis, glycolysis, gluconeogenesis and glucose uptake regulation are affected by MET, in the liver [83].

The functions of the insulin receptor and insulin receptor substrate 2 (IRS2) are enhanced by MET. Besides, glucose transporters translocation as GLUT-1 (SLC2A1) increasing cause glucose uptake enhancement to the plasma membrane [84]. Consequently, insulin-mediated suppression of gluconeogenesis enhances by MET [85]. In addition to that MET withstand to glucagon for its gluconeogenic action and this feature is of great importance [85–87]. To conclude, MET inhibits enzymes that be assigned in gluconeogenic pathway and changing multiple enzymes activity stimulates glycolysis because of MET. Gluconeogenesis constitute a 28–97 percent rate of total hepatic glucose for nondiabetic individuals based to their diet, this ratio shows an increase in patients who has type 2 diabetes mellitus [88]. This hepatic glucose rate reduce up to 75 percent by MET For T2DM patients [89]. MET reduce lactate and alanine as a substrate for gluconeogenic uptake, probably metformin-stimulated Cl– efflux is depolarized to hepatocyte membrane [90]. Despite, glycogen synthesis is decreased by hepatocytes treatment as an *in vitro* by use MET, but still it is not well-explained [91].

1.7.7. Regulation of Lipid Metabolisms

One of the effects of metformin is that it improves lipid synthesis by reducing hepatic steatosis in rodents [92,93] and it demonstrated as a clinical study [94]. Further, through both oxidation of fatty acid (in the brown adipose tissue) [95] and VLDL-triglyceride uptake increase as a selectively, by lowering plasma triglycerides, MET has a beneficial effect for circulating lipids. In tissue lipid storage, fatty acid oxidation and inhibition of lipogenesis are increase due to metformin-induced reduction, probably through AMPK activation [80,95,96]. ACC1 and ACC2 were explained AMPK phosphorylation insensitive in knocking mouse models. Thus provide AMPK action in the presence of MET that affects lipid metabolism [97]. That mice are resistant to MET actions which are lipid-lowering and insulin-sensitizing effects. This observations indicate which MET reduces cellular fatty acid levels, which affects MET-induced blood glucose reduction through AMPK-dependent phosphorylation of ACC (acetl CoA carboxylase). In the specific circumstance, MET action on hepatic glucose production inhibition may be secondary to the drug effects on ACC [81]. The loss of LKB1 inhibits phosphorylation of ACC and MET during metformin-induced AMPK phosphorylation, which increases insulin sensitivity and reduces blood glucose.

1.7.8. Metformin Prevents Cell Death

The permeability transition pore (PTP) channel is usually closed to keep the mitochondrial membrane potential up, that essential to ATP synthesis. PTP is found in the inner membrane of the cell. Once it is permanently free, membrane potential collapses [98], resulting in significant ATP synthesis inhibition. Also, PTP can opening other effects. PTP inhibits Complex I [99] for the ROS production via reallocating the electron flux. Further, PTP cause the mitochondrial pro-apoptotic proteins release into intact cell [100] and in mitochondria [101]. In endothelial, INS-1 insulinoma, HeLa, A375 cells and [102–105]. MET shows to PTP opening prevention. Metformin, as a consequence, endothelial cells protection from oxidative stress-induced cell death [102] and KB cells [106], etoposide in primary neurons [107], hyperfructosemia in INS-1 cells [103,108]. Also many research illustrates MET protects against oxidative stress or ischemia reperfusion damage, but none have looked into

the role of the PTP [67,109]. As endothelial cells are undergo to high-glucose levels, PTP opening and eventual cell death prevents by MET [102].

1.7.9. Metformin Action of Cancer

The MET function is related reduced cancer risk. MET exposure duration and cancer incidence associated with each other in terms of dose–response relationships, according to Josie M.M. Evans et.al [110]. Also, recent studies observed, when T2D patients treated with MET, it reduced incidence of cancer mortality and neoplastic disease [111,112] Further, some of the specific cancers shows a significant decrease when treated with MET, such as breast, prostate and pancreas [113–115]. The antiproliferative effect of MET has been shown in animal models experiments on a variety of cancer cell lines and cancers [116].

Several potential molecular mechanisms exist for explanation of MET and cancer development reduces. One of the mechanisms is the most generally on metabolic processes and inhibiting growth stimuli in cancer cells. Also, alter cancer cell growth related to insulin-dependent and -independent mechanisms. Growth factors which are IGF-1 and insulin for the stimulating of cell survival and mitogenesis and man cancer cells express these receptors [117]. Thus, MET treatment reduce IGF-1 and insulin serum level that results with growth stimulus reducing. The study shows in in vivo models, IGF-1 and insulin reductions induced via calorie restriction that reduce cancer incidence [118]. Direct retraction of glucose may induce cell death under certain circumstances that shown in vitro studies thus similar to growth factors [119]. For aerobic glycolysis require to glucose-rich environment according to Warburg effect for cancer metabolism. MET treatment reduces hyperglycemia and any related growth advantage in susceptible tumors [120].

LKB1/AMPK inhibition by MET causes tumor cell death by lowering ATP levels, rendering susceptible cells incapable of reacting to energy stress [121]. Fatty acid synthesis regulation depending on AMPK activation by MET that causes anticancer effect via fatty acid synthase (FAS) mechanisms on several cancer cells containing colon, prostate and breast cancer cells [122]. Further MET may effect cancer cells, endothelial cell migration and angiogenesis inhibitions effect limiting tumor growth and metastasis through AMPK-dependent reductions in growth factor that are PAL-1 and VEGF (vascular endothelial growth factor) [123].

Another anti-tumor effect of metformin is through AMPK/LBK1/TSC signaling pathway. MET suppress mTOR Rag GTPase-dependent activation which results in inhibition of mTOR signaling pathway [124]. Also, MET inhibits mTOR as an AMPK- independent through up-regulating the REDD1 expression lead to cell cycle arrest [125,126]

MET reduce insulin and insulin like growth factor 1 (IGF-1) that is associated to indirect mechanism in anti-cancer function [127]. Metformin inhibits cell growth by lowering total insulin levels, which in turn decreases free IGF-1. Metformin inhibits hepatic gluconeogenesis, and is a key component of the indirect anti-cancer process [128]. Furthermore, Furthermore, MET has anti-tumor activity through CD8+ T cells [129] that key components of tumor immunity [126,130].

1.7.10. Metformin Effect on Endocytic Cycle

Metformin appears to interact with organelle Na1/H1 exchangers (eNHE) and V-type-ATPase (V-ATPase) according to two recent reports [131,132], implying the metformin activity might well be mediated via the late endosome/lysosome. The hypothesis of activation of AMPK and inhibition of mTORC1 is important since a connection among late endosome/lysosome through MET effects can be found. Metformin influences mitochondrial function, nucleus (gene transcription), and late endosome/lysosome function by molecules mentioned. According to studies which demonstrated in *C. elegans* and *Droshophila*, in conjunction with some other focused on the effect of eNHEs, metformin may regulate endosomal-lysosomal trafficking via affecting eNHEs and control late endosomal/lysosomal activity [133].

LKB1 is translocated to late endosome/lysosome membranes in response to starvation. LKB1 phosphorylates and activates AMPK, that starts off essential processes that keep the cellular energy level in control [134]. Rheb activates the mTORC1 complex on the late endosome/lysosome membranes under nutrient-rich circumstances. Starvation prevents the activation of mTORC1 from the late endosome / lyosome [135]. V-ATPase inhibits LKB1, causing mTORC1 to be released and simulating starvation, to the late endosome / lysosome. Primary metabolism regulators appear, persists or deviate by way of the late endosome/lysosome based on the energy state of the cell. In addition, its location in late endosome/lysosome is important for the determination of the activity levels, creating the

belief that late endosome/lysosome detects the cell's energization status and establishes the key metabolic regulators activity. MET activates AMPK, inhibits V-ATPase inhibition also inhibits mTORC1. In the same manner with V-ATPase inhibition, Metformin imitates starvation. One hypothesis would be which MET changes late endosomal/lysosomal stiation from nutrient rich to starvation, maybe through influencing proteins in late endosome/lysosomes like Na1/H1 or V-ATPase [131,132].

The easiest way to regulate the endosomal cycle for metformin is to adjust the pH of the endosomes with eNHE or V-ATPase. Due to pH changes, the gradient within endosomal organelles can enhance and in particularly accelerate endocytic cycles. One of the effects of a long endocytic cycle is the quick insulin receptors recycling or glucose transporters by recycling endosomes. It was found to increase insulin sensitivity by merely increasing the GLUT-4 in muscle membrane. The endocytic cycle may further boost the performance of the lysosome, degradation of promote and cellular waste recycling [136].

This shows that pH changes in endosomes and lysosomes can influence aging and mitochondrial function. Metformin may have a range of positive effects on the cell through modifying endosome compartments pH like late endosomes also lysosomes. Besides, AMPK direct activation or mTOR inhibition via switching late endosome/lysosome states. Metformin can play role on cell metabolism through affecting the rate the endocytic cycle to receptor and transporter and autophagy [133].

1.8. 6-MERCAPTOPURINE

1.8.1. History of 6-Mercaptopurine

It was discovered in 1948, it has been approved for using human medical and FDA (Food and Drug Administration) accepted 6-MP as an antitumor drug in 1953 [131]. After that, 6-MP was used to cure ulcerative colitis (1962) and Crohn's disease (1963). (1969) [132], [133]. 6-mercaptopurine monohydrate (MP·H2O) is commercially form. In water, it has low solubility, which is 0.135 mg/mL for this reason its oral bioavailability is low about 16 percent [130].

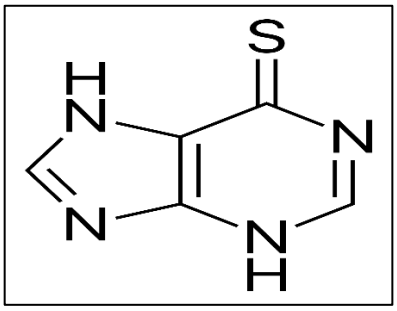

Figure 1.6. Molecular structure of 6-MP

6-MP derivated from azothiopurine (AZA) which is a prodrug and azothiopurine is non-enzimatically transformed to 6-MP and S-methyl-4-nitro-5-thioimidazole, in tissue [137]. Since AZA has a molecular weight of 55 percent that of 6-MP and 88 percent of AZA is transformed to 6-MP, a conversion factor of 2.08 must be used for comparing equal doses of 6-MP and AZA.

As an antineoplastic, immunosuppressant and antimetabolite drug is 6-mercaptopurine which use for treatment of human leukemia (ALL), rheumatoid arthritis and lupus erythematosus [138,139]. It is also used for non-Hodgkin-lymphoma, polycythemia vera, systemic lupus erythematosus and inflammatory diseases like Crohn's syndrome and ulcerative colitis when 6-MP combination with other drugs [137,140].

1.8.2. Mechanism of 6-Mercaptopurine

Potential immunosuppressive effect of 6-MP showed on antigen injected animals that treated with 6-MP, obtained results show antibody response development prevention established by Schwartz et al. [141]. DNA, RNA and protein synthesis inhibitions and also effects of reactive thiol group cause immunosuppressive and cytotoxic effect of 6-MP.

6-MP and also azothiopurine interferes involve biochemical pathways via using with endogenous purine (central components of DNA, RNA and some co-enzymes) [142]. In erythrocytes, glutathionyl imidazole and 6-MP occurs through once administered AZA is cleaved via nonenzymatic reaction [143].

6-MP has immunosuppressive features that conceivable regulated by its involvement with nucleic acid metabolism and protein synthesis in the series following antigen stimulation, and via its cytotoxic activity on lymphoid cells [144,145]. This cytotoxicity against lymphoid cells provides to 6-MP using leukemia and lymphoma treatment. Into a ribonucleotide, 6-MP must be transformed intracellularly because it is not active. Via the xanthine oxidase enzyme, 6-MP is catabolized and transformed to 6-thiouric acid in the intestinal mucosa and liver [142]. 6-MP exact bioavailability ranges from 5-37 percent as proof [146]. 6-MP anabolic transformation of active metabolites occurs intracellularly through hypoxanthine phosphoribosyl transferase (HPRT) and thiopurine methyl-transferase (TPMT), resulting in 6-methylmercaptopurine (6-MMP), 6-methylthioinosine 5'-monophosphate (6-Me-tIMP), and 6-thioguanine nucleotides (6-TG). TPMT activity shows a genetic polymorphism. Increased cytotoxicity has been associated with low TPMT activity, through the metabolism of 6-MP to be shunted towards the excessive 6-TG nucleotides production [147].

Active and inactive end products of 6-MP obtained via several enzymatic pathways. There are three key enzymes for 6-MP metabolism which are xanthine oxidase (1), hypoxanthine phosphoribosyltransferase (2) and thiopurine methyltransferase (3). Hepatocytes and enterocytes contain a high concentration of xanthine oxidase. 6-thiouric acid, an inactive metabolite, is occurred by xanthine oxidase which converts 6-MP. Xanthine oxidase, the first pass catabolism of 6-MP, provide oral bioavailability reduces of drug as a significantly. 6-MP biotransformation to its active metabolite (6-thioguanine nucleotide/6-TGN) carried out by hypoxanthine phosphoribosyltransferase as a second key enzyme of 6-MP metabolism6-MP and the intermediate of the hypoxanthine phosphoribosyltransferase pathway, which is converted to methylmercaptopurin.e ribonucleotide and 6-methylmercaptopurine, which are inactive metabolites, by thiopurine methyltransferase (TPMT) [148].

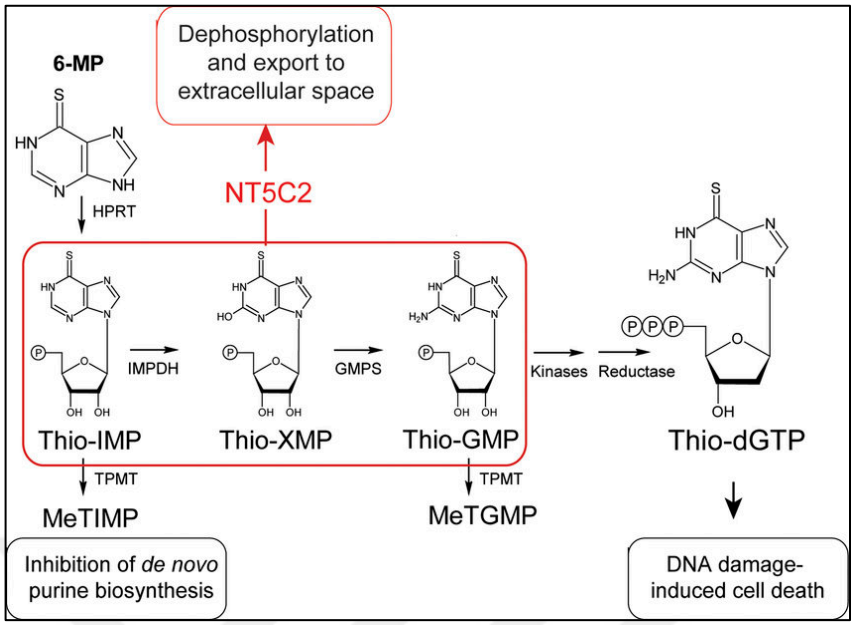

Figure 1.7. Schematic representation of 6-MP mechanisms [149]

Immunomodulatory and anti-inflammatory exact molecular mechanisms of 6-MP and AZA are unknown however presumably it occurs through several mechanisms. 6-TGNs active metabolites interfering chromosomal replications and synthesis of RNA and DNA [142]. T and B lymphocytes proliferations inhibited by 6-MP and AZA. Drugs interfere with the cytotoxicity of T and B cells then reduce cell-mediated immunity and suppressor T-cell function [142,145]. According to the latest evidence, drugs, immunosuppressive properties occur via inducing T-cell apoptosis [148,150].

Lymphoblastic leukemia (ALL) survival rates have significantly increased by 6-MP antimetabolite [151–153] The primary thiopurine cytotoxicity metabolism causes 6-thiodeoxyguanosine (dGS) nucleotide incorporation into DNA in proliferating cells [154,155] that leads to two effects. First effect is dGS insertion into DNA accounts for altered DNA-protein interactions [156,157]. The second effect, thiopurine cytotoxicity is promotes by the DNA mismatch repair system (MMR) via initiating a cycle of futile efforts to repair DNA lesions which including thioguanine mismatch pairs [158,159].

Cytochrome c amount, which released into the cytosol, extremely enhanced with 6MP treatment in Leydig cells [160]. 6-MP increased Bcl-XL expression in Leydig cells treatment. Further, the toxicity of 6-MP related to ROS production. Thiouric acid occurs by cytosolic xanthine oxidase through to 6 MP metabolization that process has the potential to

form ROS (reactive oxygen species) especially H_2O_2, in some cell types [161]. The study investigates the ROS mechanism in the presence of 6-MP. This study result demonstrates ROS produces by 6-MP and that important step in eliciting Leydig cell death [160].

6-MP stimulates the caspase pathway. Leydig cells were immune to the cytotoxic effect of 6 MP when caspase 9 inhibition (by Ac-LEHD-CHO, abbreviated LEHD) or pan-caspase inhibition (by ZVAD-FMK, abbreviated ZVAD) was used. To verify that it was involved, researchers examined to see whether a caspase 3 target, PARP, was cleaved in Leydig cells. Immunoblot study using an antibody that directly recognizes cleaved PARP reported enhanced cleavage in 6 MP treated cells, indicating caspase 3 activation. Inhibition of caspase 3's upstream activator, caspase 9, also prevented PARP cleavage caused by 6 MP. Surprisingly, caspase inhibition had no effect on 6 MP-induced ROS development. Overall, these results suggest that although 6 MP produces ROS, it is incapable of eliciting death on its own and needs caspase 3 activation as well.

According to the study cell death by 6 MP generated ROS: Xanthine oxidase generates thiouric acid via metabolization of 6-MP. By acting on mitochondria through cytosolic ROS (suppressed by NAC), this causes cytochrome c release in a BAK-independent way. The apoptosome is a complex that recruits pro-caspase 9, which is then auto-activated [162]. After that, triggered caspase 9 cleaves pro-caspase 3, initiating a cascade of events that culminate in cell death, including PARP cleavage. Leydig cell death is aided by thiopurine nucleotide triphosphates of 6 MP. Apoptosome activation is enhanced by thiopurine nucleotides. Thiopurine nucleotides enhance apoptosome assembly [160].

Acording to study, leydig cell death via 6-MP induced require two pathway. One of them, cytosolic ROS productions with thiouric acid by 6-MP metabolism, generating cytochrome c release. Thiopurine nucleotides, which produce via 6-MP metabolization, are incapable for apoptosome activating. Thiopurine nucleotides are incapable apoptosome activation, also its are 6-MP metabolits [160].

6 MP is divided into nucleotides of thiopurine which cannot cause their apoptosome alone. When filled with dATP, however, Apaf-1 takes the form that makes it easier to bind thiopurine nucleotides. This new mechanism for activation of apoptosome demonstrates the importance of the relationship among concentration of thiopurine nucleotide and dATP in

that new cell death mechanism. Ultimately, exports by MRP4 would prevent apoptosome activation of thiopurine nucleotides.

6-MP has antiproliferative effects via various mechanisms in terms of de novo purine synthesis inhibitions and ability to DNA damage and its leading to apoptosis (through to incorporation into nucleic acids chains) [163]. ATP and GTP de novo biosynthesis are inhibited by 6-MP [164]. 6-MP may interfere with impact metabolic reprogramming and metabolic checkpoints due to phosphatidylinositol 3 kinase (PI3K) / mammalian target of rapamycin (mTOR) signaling pathway is inhibited by drug in cancer and T cells [165,166].

1.8.3. Thiopurine Methyltransferase Enzyme (TPMT)

6-thioguanine which is cytotoxic nucleotide metabolites and TPMT activity have reciprocal relation in leukemic children's erythrocytes when they taking 6-MP. Correspondingly, this may cause competition between the 6-thioguanine nucleotides formations through to separate pathways and TMPT catalyzed metabolic pathways. In other words, the higher TMPT inherited activity fewer 6-MP is suitable to transformation for active nucleotide metabolites [142].

6-MP catabolized by thiopurine methyltransferase (TPMT). 6-MP convert to inactive 6-methylmercaptopurine (MMP) as a result of this catalysis. Low activity of TPMT interprets (translates) in higher erythrocyte concentrations of 6-thioguanine nucleotides (TGNs) which are 6-MP active metabolites. In ALL patients, lower possibility of disease relapse and hematopoietic toxicity such as neutropenia correlate with higher TGN concentrations [167]. TGNs could converted to contain thioguanine (TG) also thioguanosine (rTG) that are thiopurine bases through acid-hydrolyzed [138].

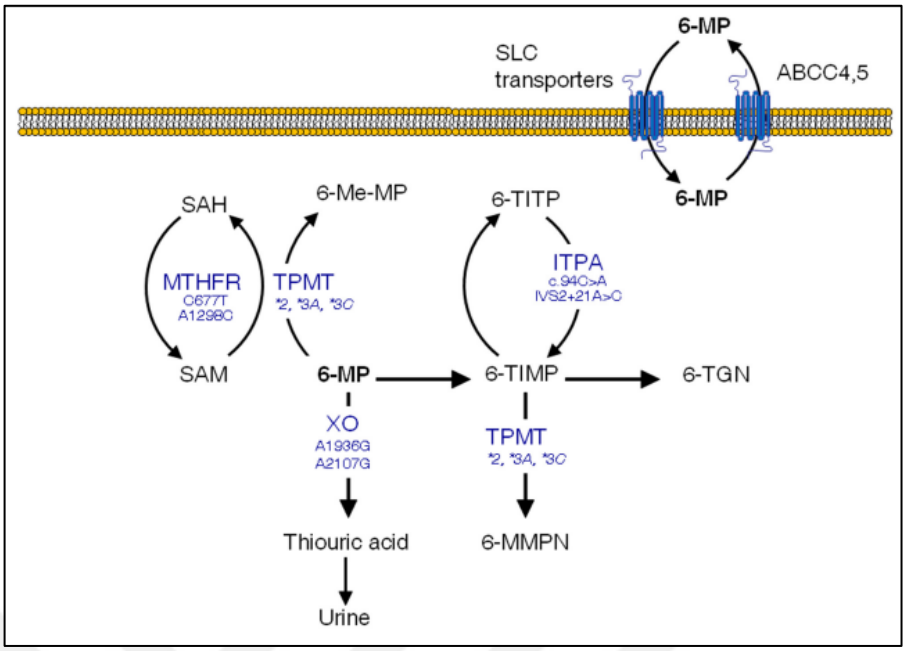

Figure 1.8. Polymorphisms in the 6-MP intracellular pathway have been related to an adverse effects increased risk [168]

TPMT activity causes the wide interindividual differences due to widespread genetic polymorphism [169]. S-methylation catalyze is the major catabolic pathway of 6-MP through the thiopurine methyltransferase enzyme. Common genetic polymorphism causes a variety of TPMT activity in Individuals [170]. High TPMT activity (TPMTH) for an allele shows homozygous roughly 89 percent of the population, however low TPMT activity (TPMTH) for an allele shows homozygous roughly 1 percent of the population, in 300 subjects. Heterozygous (TPMTH/TPMTL) and intermediate consist of 11percent of population [169].

1.8.4. *De Novo* Purine Synthesis Inhibitions of 6-Mercaptopurine

For inhibit de novo purine synthesis within a cell, methylatedthioinosinic acid (MeTIMP), active form, catalyzed by hypoxanthine phosphoribosyltransferase (HPRT) as a first metabolized of 6-MP [171]. Then it was translated into a DNA intercalating agent called 6-thioguanine (6-TG). As a result, 6-TG incorporation causes cytotoxicity via G2/M and/or S phase arrest [172]. XO (Xanthine oxidase) and TPMT (thiopurine S methyl transferase) complex biotransformation 6-MP that causes incomplete and variable bioavailability

(approximately 16–50 percent) and restricts 6-MP bioavailability [173,174], plummeting chemotherapeutic impact and life-threatening toxicity [137,142,175].

1.8.5. Anticancer Effect of 6-Mercaptopurine

In biological system, 6-MP is an anticancer-inactive. But through to enzymatic reactions, 6-MP can be converted into anticancer-inactive as an intermediate. Those enzymatic reactions for prevent cancer cells replications via include into DNA and RNA sequences [55]. First 6-MP transformed to 6-thioinosine monophosphate (6TIMP,) after to 6-mercaptopurine-ribose (6MPR) under the hypoxanthine guanine phosphoribosyl transferase (HGPRT) catalysis, can be shown as proven examples [176].

2. MATERIALS

2.1. CHEMICALS AND REAGENTS

Dulbecco's Modified Eagle's Medium (DMEM), fetal bovine serum (FBS) and Trypsin-EDTA/0.25 percent were purchased from Sigma-Aldrich/Germany. Penicillin&Streptomycin/10,000 U/mL and phosphate buffered saline (PBS) were purchased from Gibco/UK. WST-1 Cell Proliferation Reagent were obtained from Roche Diagnostic GmbH/Germany. Metformin and 6-mercaptopurine were obtained from Sigma-Aldrich/Germany. $HAuCl_4 \bullet 3H_2O$ was supplied from Sigma-Aldrich/Germany. $C_6H_5Na_3O_7$ were acquired from Merck Millipore/Germany.

2.2. INSTRUMENTS

Instruments used for this study is that UV/Vis spectrometer from PerkinElmer/USA, Zetasizer Nano-ZS (dynamic light scattering (DLS)) from Malvern Insturements/UK, Raman microscopy system from InVia Reflex, Renishaw/UK, ELx800 Absorbance Reader from Biotek/USA, Esco Class II type Biohazard safety cabinet from A2/USA and CO2 incubator (37ºC, CO_2 5 percent) from Nuaire/USA.

2.3. CELL LINES

A549 (human epithelial lung carcinoma) and Beas-2b (human epithelial bronchus) cell lines were received from American Type Culture Collection (ATCC)/USA.

3. METHODS

3.1. GOLD NANOPARTICLES SYNTHESIS

Average size of 50 nm spherical AuNPs were synthesized by Turkevich method as a known citrate reduction method [177]. Before starting the synthesis, HCl:HNO_3 of 3:1 (aqua regia) used for washing and surface cleaning of glasses which are used for gold nanoparticles synthesis. Under continuous stirring, 10 mg of $HAuCl_4$.3H2O in 100 mL dH2O was heated to boil. Thereafter, 0.8 mL of one percent $Na_3C_6H_5O_7$ was added quickly. The boiling AuNPs solution was allowed to cool at 25°C after 15 min. AuNPs stored in the dark at room temperature.

3.2. GOLD NANOPARTICLES CHARACTERIZATIONS

AuNPs were characterized via UV-Vis spectrophometer. Hydrodynamic size measurements of the 50 nm AuNPs were measured using Zetasizer Nano-ZS at the room temperature at 173°C scattering angle with a 4 mW He–Ne laser.

3.3. CELL CULTURE

Beas-2b cells were grown in high glucose DMEM with 5 percent FBS, and 1 percent P&S A549 cells were grown in DMEM/F-12 including 10 percent FBS and 1 percent P&S. Cultured conditions was 37°C under 5 percent CO_2 humidified atmosphere for the cells.

3.4. WST-1 CELL PROLIFERATION ASSAY

$12x10^3$ Beas-2b or A549 cells were seeded on 96-well plate incubated for 24 h which allows attachment of the cells. Afterward, cells were exposed with 2.5, 5, and 20 μM MET or 0.5, 2.5, and 15 μg/ml 6-MP. After 24 hours, drug including medium were replaced with 5 percent WST-8 reagent in cell medium. Following 2 hours incubation with WST-8 reagent, absorbance of formazan formed by reduction of tetroazolium salts was measured at 450 nm

using by ELISA reader. 10 percent DMSO was used as a positive control. The two-paired Student's t test was used as * for $p \leq 0.05$, ** for $p \leq 0.01$, ***for $p \leq 0.001$.

3.5. SERS MEASUREMENTS

15.000 Beas-2b or A549 cells/well were seeded on CaF_2 slides in 24 well plate and incubated for 24 hours to attachment of cells. Then, cells were treated with 50 nm AuNPs for 24 hours. Following 24 hours, cells were treated with increasing concentration of MET or 6-MP in the presence of 50 nm AuNPs for 24 hours. Then, cells on CaF_2 slides were washed with PBS once, then CaF_2 slides were moved on the polydimethylsiloxane (PDMS) coated petri dish to suppress polystyrene peaks from petri dish. 20 µL cell culture medium was added on CaF_2 because these cells were not fixated and they were alive. The medium prevented cells from drying during SERS measurement under the laser.

Using a Renishaw InVia Reflex Raman Microscopy System and Leica 20x long distance objective (N.A=0.40) all measurements were performed. 830 nm photodiode laser source with 1200 line/mm grating was used to acquire the SERS spectra by mapping the cells. The laser power was 150 mW and the exposure time was 2 sec. The spectral acquisition range was set to 1471-471 cm^{-1}. The laser spot size was calculated as approximately 2.5 µm on the sample according to 1.22 ƛ/NA formula. For mapping, step size was chosen as 2 µm which is resulted as approximately 45 spectrum per cell. The average spectra of each treatment were obtained from 90 cells with three replications. Wire 4.1 software used for processing subtracting baseline, cosmic ray removal, smoothing and normalizing 1 for SERS spectra.

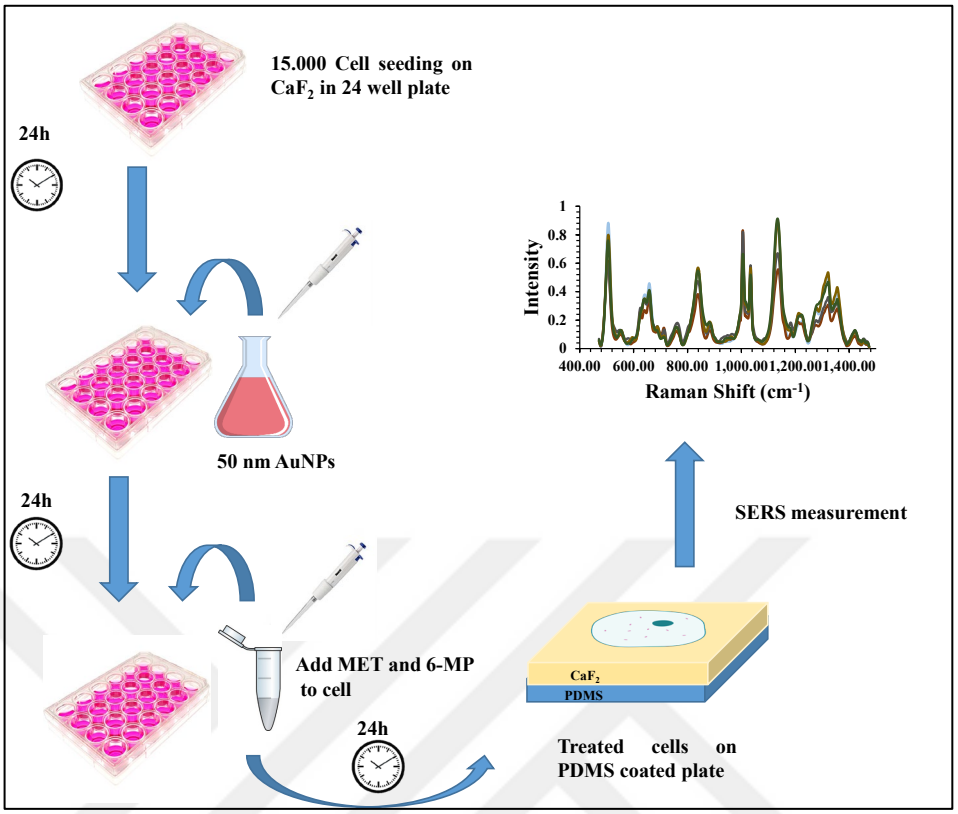

Figure 3.1. Experimental design of treatment and SERS measurements.

3.6. STATISTICAL ANALYSIS

The PCA (principal component analysis) performed to the average SERS spectrum from 90 cells per treatment group has explained SERS spectrum variation. The two-paired Student's t test was used as * for $p \leq 0.05$, ** for $p \leq 0.01$, ***for $p \leq 0.001$.

4. RESULTS AND DISCUSSION

4.1. CHARACTERIZATION OF GOLD NANOPARTICLES

Characterizations of 50 nm AuNPs were obtained using UV/Vis spectroscopy and DLS.

4.1.1. UV/Vis Spectroscopy

The absorbance of 50 nm average size of AuNPs were observed by UV/Vis spectrometer. According to the literature the standard wavelength of 50 nm AuNPs is 532 nm [178]. The absorption band of 50 nm AuNPs was obtained at 530 nm as seen in figure 4.1.1.

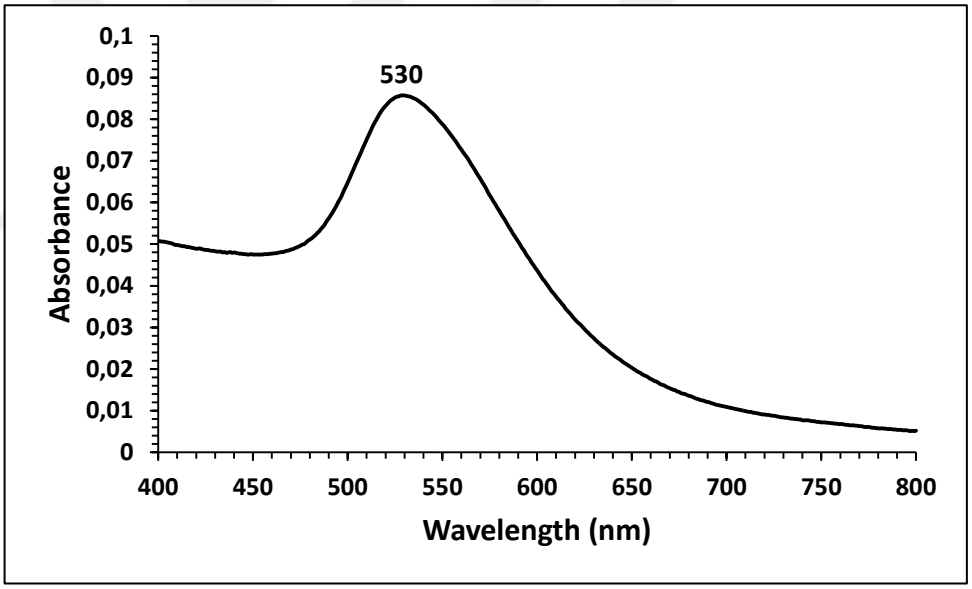

Figure 4.1.1. UV-Visible absorbance spectrum of AuNPs

4.1.2. Dynamic Light Scattering

The average hydrodynamic size of AuNPs was measured 50 nm using DLS shown in figure 4.1.2. Explanation of the 50 nm AuNPs is that citrate ions which associated with nanoparticles surface measuring together AuNPs by DLS consequently the hydrodynamic size of AuNPs was measured larger than the 50 nm AuNPs.

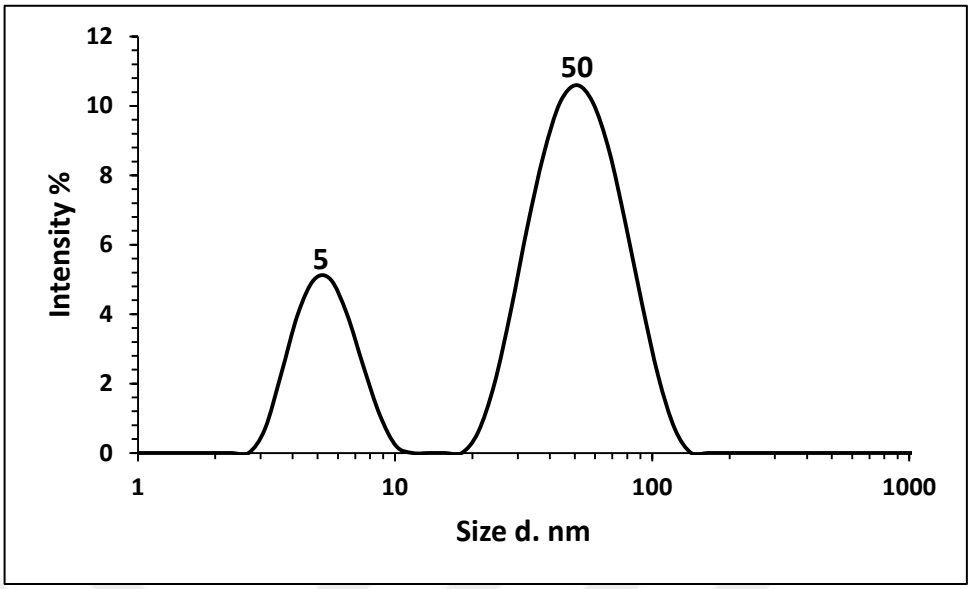

Figure 4.1.2. DLS spectra of suspension of AuNPs

4.2. WST-1 CELL PROLIFERATION ASSAY

The cytotoxicity of MET was analysed by WST-8 cell viability assay. Fig. 4.2.1. Shows WST-8 cell viability assay results of Beas-2b and A549 cells exposed with 2.5, 5 and 20 μM MET. 10 percent DMSO was used for positive control. There is not any cytotoxic effect of MET on Beas-2b cells while it induced a dose dependent toxicity on A549 cells. Especially, at 20 μM MET concentration, viability of A549 cells were decreased up to 52 percent. A high dose of MET decreases hepatic gluconeogenesis and suppresses mTOR signaling causing the inhibition of cancer cells proliferation [57,61,116,179–184].

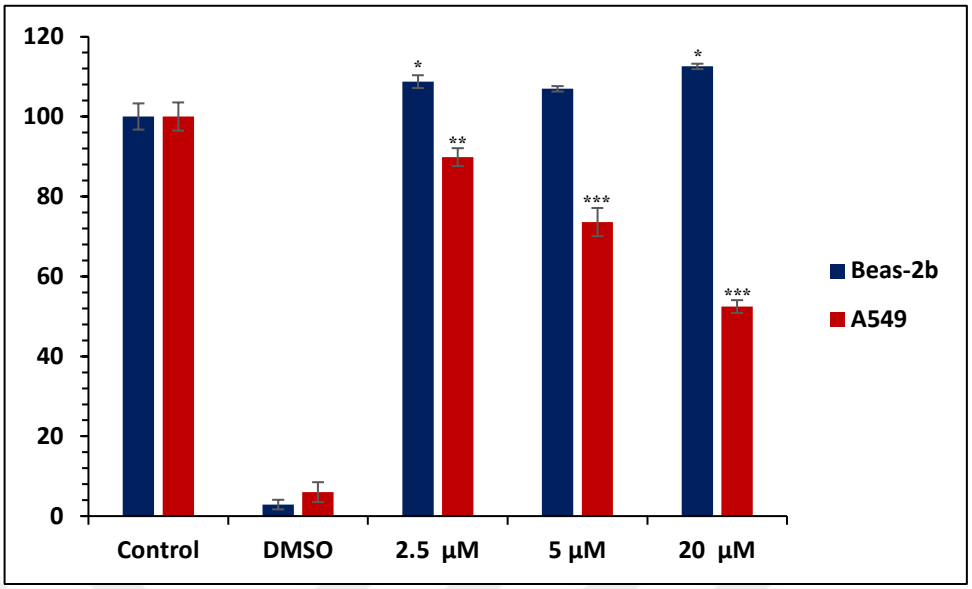

Figure 4.2.1. WST-8 cell proliferation assay of Beas-2b and A549 cells treated with different concentrations of MET. (* for p≤0.05, ** for p≤0.01, ***for p≤0.001)

Figure 4.2.2. shows WST-8 cell viability assay results of Beas-2b and A549 cells exposered with 2.5, 7.5 and 15 µg/ml 6-MP. Again, 10 percent DMSO that was used as a positive control. 6-MP has significant cytotoxic and antiproliferative effect on both Beas-2b and A549 cell lines due to the inhibitory effect on *de nova* purine synthesis.

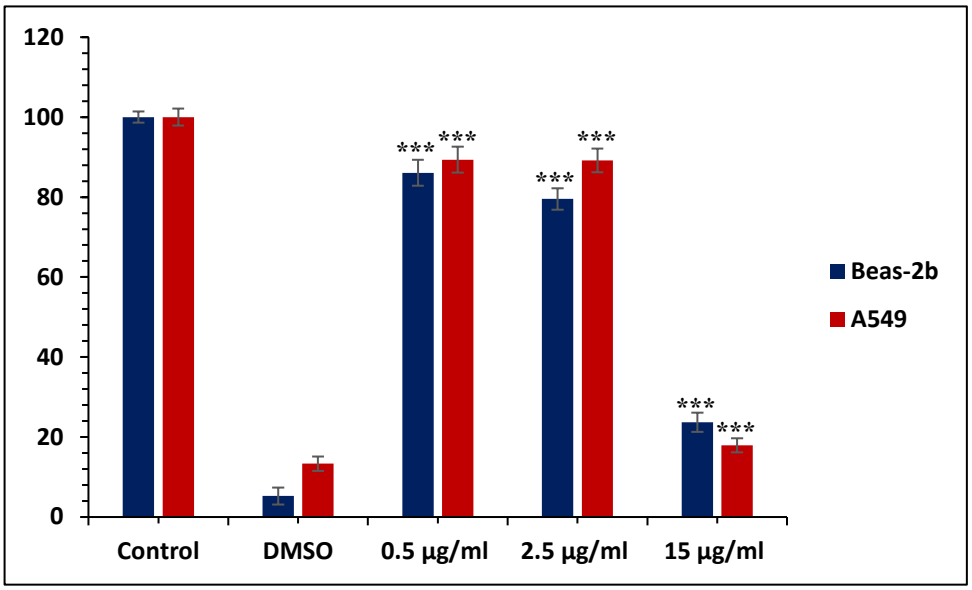

Figure 4.2.2. WST-8 cell proliferation assay of Beas-2b and A549 cells treated with different concentration of 6-MP. (* for p≤0.05, ** for p≤0.01, ***for p≤0.001)

4.3. SERS MEASUREMENT

The molecular mechanisms of drugs in the presence of 50 nm AuNPs in single-cell were analyzed using SERS. Beas-2b and A549 cells were exposed with 50 nm AuNPs. After 24 h treatment of AuNPs, cells were exposed with MET and 6-MP during 24 h and in the presence of 50 nm AuNPs. Subsequently, SERS spectra of 30 MET and 6-MP treated Beas-2b/A549 cells were collected, separately. This process was repeated in three times. Intensities of SERS spectra and obtained spectral information from the drug treated single cells changed depending on drugs molecular mechanisms.

Endocytosis is the mechanism via that nanoparticles are introduced into living cells. That is achieved by merely applying NPs to the serum media. AuNPs are taken up by early endosomes through aid of cargo proteins and lipids [185]. The vesicular bud matures can fuse with endolysosomes, forming AuNP dimers and trimers. In the meantime, proteins and receptors, especially cysteine-rich proteins, has major role in these processes [186]. Endosome maturation and AuNP aggregation status may be responsible for the observed spectral changes. Spectral variations which seen with both drugs, also due to endosomal dynamic changes induced by AuNPs accumulation state in the cell. According to this, spectral changes can explain with the mechanism of the drug as well as the changes in the endosomal pathways.

Cancer cells are normally glycolytic (Warburg effect), they are unlikely to be vulnerable to mitochondrial poison. Cells are supposed to generate mitochondrial ATP as they absorb oxygen at the mitochondrial level. This makes mitochondrial ATP production still exists even as the share of mitochondrial ATPs released in cancer cells is lowered, and this decrease may be detrimental. This inhibits cell proliferation with glucose in HCT116 p53 cells / cancer cells and stimulates cell death without glucose. Furthermore, overexpression of the MET-resistant NADH dehydrogenase NDI1 in Saccharomyces cerevisiae completely blocks the MET effect, demonstrating that metformin toxicity is largely based on its effect on Complex I. It's also possible that cancer cells have more MET accumulation or Complex I sensitivity to MET than normal tissues (personal hypothesis), and that these hypotheses have yet to be tested. [67]. As previously mentioned, MET inhibits cancer cell proliferation. As a result, it's linked to SERS spectra results. According to SERS results, MET that has different effects on normal and cancer cells. Although the effect on cancer cells of MET is

higher than on normal cells, the SERS intensities of normal and cancer cells differ from each other.

The SERS spectra obtained from Beas-2b cells are presented in Figure 4.3.1. It was found that obtained spectra have changed in the intensity for the treatment of increasing concentrations of MET**.** Intensity of 500 cm^{-1} -disulfate (S-S) bond vibration-, 655 cm^{-1} -amino acid methionine-, 1000 cm^{-1} -Phenylalanine-, 1030 cm^{-1} -Phenylalanine of collagen- peaks have changed compared with control groups. Further, intensity of 830 cm^{-1} -nucleic acids-, 1180 cm^{-1} -Cytosine/guanine-, 1222 cm^{-1} -nucleic acids, Cellular nucleic acids-, 1350 cm^{-1} -Guanine- have changed after the MET treatment. The overall changes in AMPK activation are increased presence of MET. Activated AMPK causes inhibition of mTOR1 that is resulting inhibition of cell proliferation and protein synthesis [187]. The hypothesis is intriguing as that suggests a causal link among late endosome-lysosome and MET actions of AMPK and mTORC1 inhibition. Metformin is affected by the molecules mentioned above on mitochondrial activity, nucleus (gene transcription), also late endosome/lysosome function [133]. 1130 cm^{-1} -Phospholipid structural changes-, 1270 cm^{-1} -Typical phospholipids-, 1310 cm^{-1} -lipid/collagen- peaks intensities have changed. These peaks change may occur due to the reducing of hydrophobic amino acid in membrane structures. MET cause inhibition of lipids and reduce gluconeogenesis [140,143]. Another reason of lipid changes can for the MET effect of inducing apoptosis. In several human cancer cells, MET induces apoptosis. MET induces caspase 3 activation (key molecule for the executes apoptosis) that results of apoptosis promotes [126,188,189]. Morphological changes in apoptotic cell death are characterized by blebbing of plasma membrane, nuclear fragmentation, chromatin condensation, and apoptotic body creation [190,191]. Another explanation of that changing is that MET effect on endosome. Metformin can influence endosomal pH through attacking eNHE or V-ATPase, which is the clearest way for it to regulate the endocytic cycle. That changes in pH in endosomes and lysosomes may effect mitochondrial function. Metformin may have a number of possitive effects on the cell via modifying the endosomal compartments pH as well as lysosomes also late endosome. Metformin can influence cell metabolism via affecting endocytic cycle rate for receptor and transporter trafficking and autophagy, as well as directed activation or suppression of AMPK and/or mTOR by flipped the late endosome/lysosome states [136, 192]. According to the t-

test results, the amino acid methionine, nucleic acids, cytosine/guanine, nucleic acids, typical phospholipids and guanine peaks changed significantly.

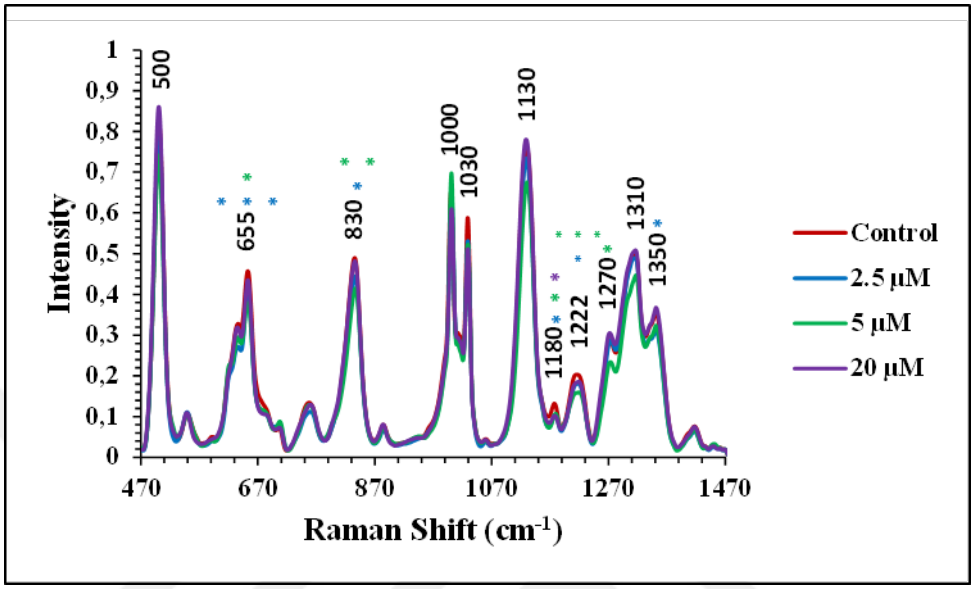

Figure 4.3.1. Average SERS spectra of Beas-2b cell line at increasing MET concentrations (* for p≤0.05, ** for p≤0.01, ***for p≤0.001, *: represent to 2.5 µM, *: represent to 5 µM, *: represent to 20 µM)

PCA (principal component multivariate analysis) is use for large data set to identify major changes of basis on the data. For this reason, PCA suitable for discriminating large changes in SERS spectra derived from biomolecules. In this study, PCA was utilized for the SERS spectra of each control, MET and 6-MP treated cells.

Figure 4.3.2. Represents comparison of the major variations of first and second PCs of control and MET treated Beas-2b cells. The PC1 scores comparison of control and MET treated cells was illustrated in figure.4.3.2 (a) The most significant positive contribution after MET treatment were observed of peaks 500 cm^{-1} -ν(S-S) gauche-gauche-gauche-, 1145 cm^{-1} –Glycogen-, 1310 cm^{-1} -lipid/collagen-, 1350 cm^{-1} -Guanine-. On the other hand, negative contributions were observed from the peak is 1000 cm^{-1} -Phenylalanine-. Figure 4.3.2. (b) Demonstrates the comparison of PC2 scores of each control and MET treated cells. The positively dominating variables were observed 520 cm^{-1} -Phosphatidylinositol-, 750 cm^{-1} -tryptophan-, 880 cm^{-1} -Tryptophan-, 1145 cm^{-1} –Glycogen-. 1300 cm^{-1} –lipids- peak was

changed as a negative contribution. As it is clearly seen from the PC1 and PC2 scores, the variables of the spectra from control and MET treated Beas-2b cells were changed lipids, proteins, nucleic acids and also glycogen structures. Reason of this changes is that mechanisms of MET which AMPK, lipid, protein and glycogenesis inhibitions mechanisms.

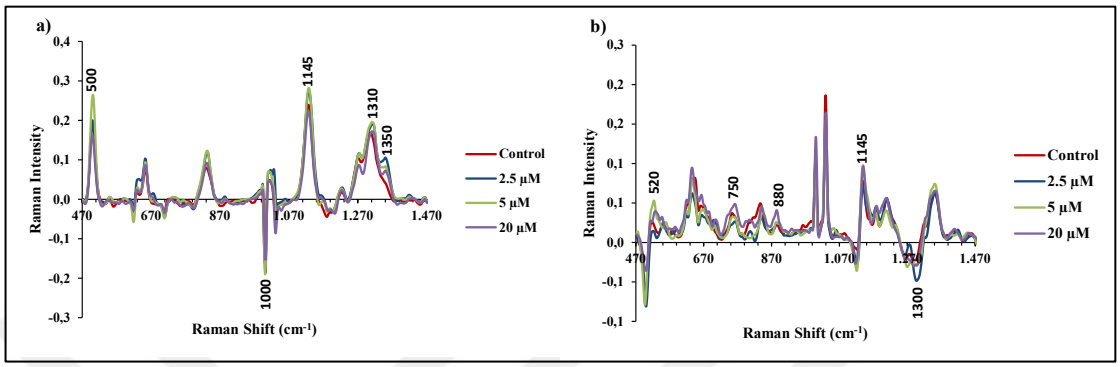

Figure 4.3.2. Comparison of (a) first and (b) second PCs of control and MET treated Beas-2b cells

On the other hand, MET have different action mechanism on the cancer cells when compare with normal cells. Cancer cells even more acidic as they produce lactic acid while healthy cells have alkaline medium. MET has positive charge, also glucose level is low, MET changes accelerating cytotoxic to cancer cells. Because of this property of metformin, it does not harm healthy cells and is toxic to cancer cells. The spectral changes during different concentration of MET treatment on A549 cells are shown in Figure 4.3.3.

500 cm^{-1}, 592 cm^{-1} and 708 cm^{-1} peaks demonstrates increase, related to ν(S-S) gauche-gauche-gauche, glycerol and membrane phospholipids, respectively. MET suppress lipid and cholesterol biosynthesis. This suppression mechanisms partially relevant to mitochondrial respiratory chain complex I as a temporary inhibition and also dependent on indirect AMPK activation [140,193]. AMPK is main regulator of lipid biosynthetic pathways because AMPK has effect on inactivation also phosphorylation of main enzymes as acetyl-CoA carboxylase (ACC) [80,194]. Another inducing effect of MET on apoptosis is that stimulating ROS production and the mitochondrial membrane potential reducing. P53 can activated and phosphorylated by AMPK, after that P53 induces cell apoptosis which happen in low nutrient conditions. As a result of MET promote apoptosis through AMPK/p53 pathway activations [126,195].

Intensity of amino acid methionine and phenylalanine of collagen peaks were decreased at 635 and 1030 cm^{-1}. Phenylalanine peak intensities increased at 1000 cm^{-1}. 926 cm^{-1} peak occurred related with protein band. Peak intensities at 667 cm^{-1}, 830 cm^{-1} and 1222 cm^{-1} originating from DNA/RNA, nucleic acids and Cellular nucleic acids changed. Moreover, intensity of guanine peaks decreased at 1316 cm^{-1} and 1350 cm^{-1}. The cause of protein and nucleic acids peaks changing is MET mechanisms. Proliferation of cells and protein synthesis in cancer cells inhibition occur when the AMPK activation mediated by mTORC1 signaling inhibition. mRNA translation regulations, Protein and de novo lipid synthesis promote by mTOR [196,197]. Also, mTOR promotes cell growth and nucleotides synthesis through protein catabolism suppression [198]. Furthermore, mTORC1 inhibits the DNA damage response cascade by inducing p53 target genes such as the AMPK regulatory subunit (AMPK), PTEN, and TSC2, which all increase TSC function [199,200]. Beside that effects of MET, also drug effects endosome mechanisms which results spectral change of proteins. Metformin, by the way, activates AMPK, stimulates mTORC1, and mimics inhibition of V-ATPase. Metformin works in the same manner as V-ATPase inhibition does in simulating starvation. Metformin, according to one hypothesis, causes the late endosomal/lysosomal state to transition from nutrient-rich to nutrient-starved, possibly via influencing proteins in late endosome/lysosome as Na1/H1 exchangers as well as V-ATPase [199,200]. According to the t-test results, the amino acid methionine, membrane phospholipids, nucleic acids, protein band, phenylalanine, cellular nucleic acids, guanine peaks changed significantly.

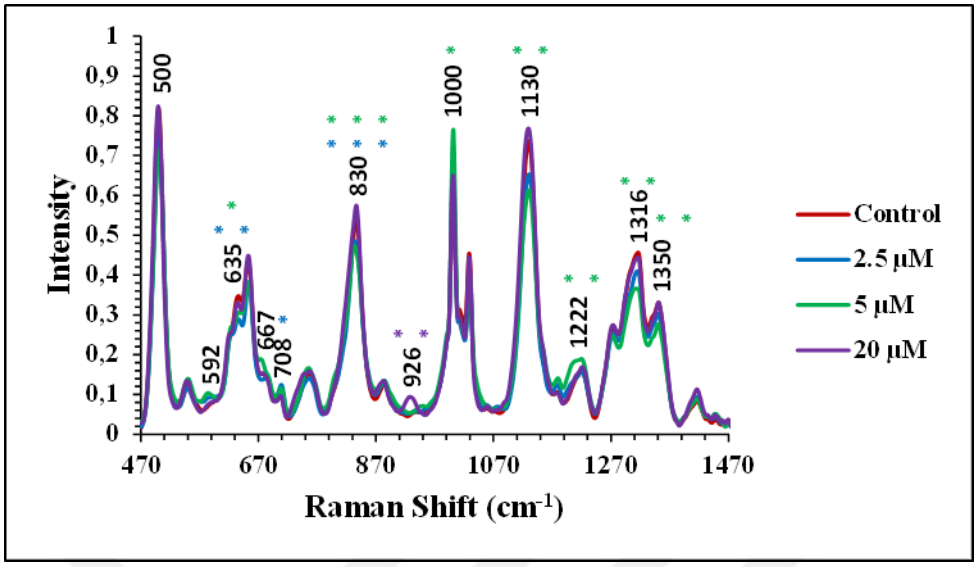

Figure 4.3.3. SERS spectra of A549 cell line at increasing MET concentrations (* for p≤0.05, ** for p≤0.01, ***for p≤0.001, *: represent to 2.5 µM, *: represent to 5 µM, *: represent to 20 µM)

Figure 4.3.4. represents comparison of the major variations of first and second PCs of control and MET treated A549 cells. The PC1 scores of control and MET treated A549 cells was illustrated in Figure.4.3.4. (a) The main differences after MET treatment achieved with positive contribution of peaks 500 cm^{-1}, 650 cm^{-1}, 830 cm^{-1}, 1130 cm^{-1}, 1310 cm^{-1} related to ν(S-S) gauche-gauche-gauche, Tyr, nucleic acids, phospholipid structural changes and lipid/collagen respectively. The negative contributions were observed at 570 cm^{-1} -Tryptophan/cytosine, guanine-, 712 cm^{-1} –adenine-, 1000 cm^{-1} –Phenylalanine-, 1035 cm^{-1} –Collagen-. The PC2 scores after the MET exposure seen in Figure 4.3.4. (b) intensity of peaks decreased compared with control at 500 cm^{-1} -ν(S-S) gauche-gauche-gauche-, 630 cm^{-1} -Glycerol-, 920 cm^{-1} -proline ring/glucose-, 1030 cm^{-1} -Phenylalanine of collagen-,1150 cm^{-1} -protein-, 1310 cm^{-1} -lipid/collagen-,1350 cm^{-1} –Guanine-. De novo lipid synthesis promotes by mTOR. MET inhibits mTOR activations. Lipid changes reason is that the mTOR inhibitions by MET treatment on A549 cells. The extent of autophagy induction is determined by mTOR and AMPK activity. mTORC1, which regulates genes expression to lysosomal biogenesis and autophagy machinery, that autophagy regulates through nuclear translocation phosphorylating and inhibiting of transcription factor TFEB [192,200,201]. These mechanisms explain the nucleic acids changes on A549 cells when cells treated with MET.

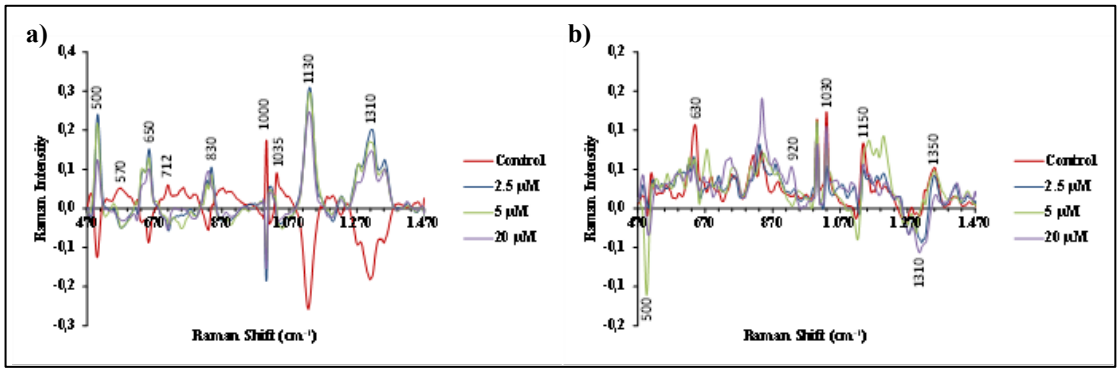

Figure 4.3.4. Comparison of (a) first and (b) second PCs of control and MET treated A549 cells

SERS spectra of Beas-2b cells when treated with increasing 6-MP concentrations illustrated Figure 4.3.5. For this reason, some peak of nucleic acid intensities is change because of 6-MP mechanisms. The significant changes about nucleic acid peaks intensities are that DNA -685 cm^{-1}- and guanine -1350 cm^{-1}-. 6-MP have effect on pathway of *de novo* purine synthesis the way of inhibition. Thus, observations changed of nucleic acid and DNA/RNA components in cells. Another explanation of this change according to endosomal pathways is that may be clarified by the development of larger AuNP aggregates within the endolysosome, which could contribute to increased activity of GTPase to have enough energy to endolysosomal protein structure control. OH out-of-plane bending and ν(S-S) gauche-gauche-gauche, glycerol, Phospholipid structural changes, typical phospholipids are changing because of its membrane structures, at 585 cm^{-1},501 cm^{-1}, 630 cm^{-1}, 1130 cm^{-1} and 1270 cm^{-1}. Changing peak of proteins are tyrosine at 835 cm^{-1} and 1175 cm^{-1}, phenylalanine at 1000 cm^{-1} and 1030 cm^{-1}. When the nucleic acids or DNA inhibits, central dogma of gene expression that include replication transcription and translation pathways is inhibited. This mechanisms results inhibition of protein synthesis [140,187,202,203]. Another point of view of that changes which there are lipids in the endosomal membrane that are aligned with the endosomal membrane identity. With the maturation of early endosomes to late endosomes, both these spectral variations mean that AuNPs association with endosomal membrane declined. Biochemical changes in endosomal vesicles dominated the observed spectral changes. According to the t-test results, the DNA, tyrosine and guanine peaks changed significantly.

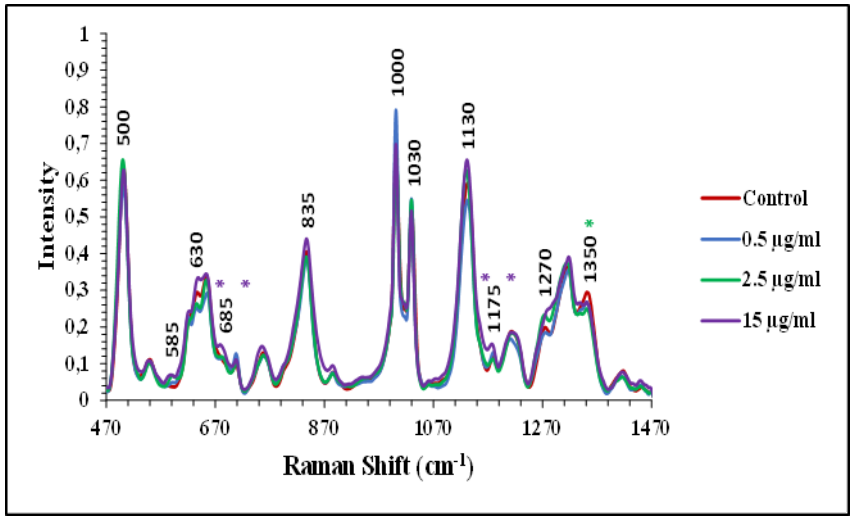

Figure 4.3.5. Average SERS spectra of Beas-2b cell line at increasing 6-MP concentrations (* for p≤0.05, ** for p≤0.01, ***for p≤0.001, *: represent to 0.5 µg/ml, *: represent to 2.5 µg/ml, *: represent to 15 µg/ml)

Figure 4.3.6. represents comparison of the major variations of first and second PCs of control and 6-MP treated Beas-2b cells. The PC1 scores of control and 6-MP treated cells was illustrated in Figure 4.3.6. (a) The primary changes after 6-MP treatment were observed peaks are 550 cm^{-1}, 746 cm^{-1}, 1000 cm^{-1}, 1310 cm^{-1} and 1425 cm^{-1} contribute to cholesterol, DNA/RNA, phenylalanine, lipid/collagen and deoxyribose, respectively. The PC2 scores of 6-MP treated Beas-2b cells was demonstrated in Figure 4.3.6. (b) important peak changes were that 490 cm^{-1} –Glycogen-, 640 cm^{-1} -proteins; tyrosine-, 674 cm^{-1} - DNA-, 750 cm^{-1} - tryptophan-, 844 cm^{-1} -polysaccharide structure-, 1000 cm^{-1} –phenylalanine-, 1030 cm^{-1} - Phenylalanine of collagen-,1140 cm^{-1} -carbohydrates-, 1350 cm^{-1} -guanine-.

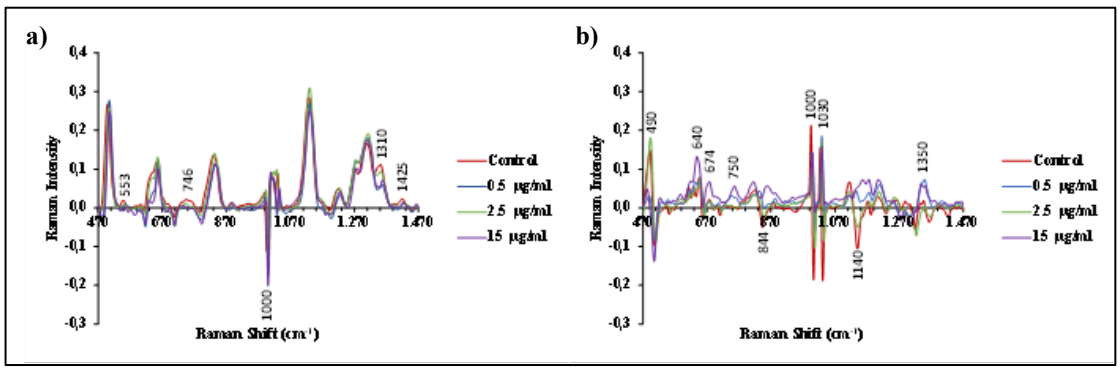

Figure 4.3.6. Comparison of (a) first and (b) second PCs of control and 6-MP treated Beas cells

SERS spectral changes of A549 cells treated with increasing concentrations of 6-MP demonstrated on Figure 4.3.7. Intensity of 500 cm^{-1} -ν(S-S) gauche-gauche-gauche-, 1130 cm^{-1} -Phospholipid-, 1310 cm^{-1} -lipid/collagen-, 1350 cm^{-1} -Guanine- changed. This may be attributable to the start of 6-MP mechanisms of apoptotic cell death pathways Phosphatidylserine (PS) localization at the external surface of the cell membrane, permeabilization of mitochondrial membrane, cytochrome-c release, activation of caspase, also cleavage of inter-nucleosomal DNA are all well-known biochemical modifications in apoptosis. 6-MP has antiproliferative effects via de novo purine synthesis inhibitions and ability to DNA damage and its induces apoptosis (through to incorporation into nucleic acids chains) [204], [163]. One of the apoptosis mechanisms is ROS releases. 6-MP has potential ROS production [160]. When that spectral changes evaluate in terms of endosome mechanism, these changes can be explained as follows: Along membrane wrapping and budding from the cell membrane, AuNPs interfere with membrane receptors. The vesicles transition from the cell membrane to the cytosol as time progresses. Besides that, early endosomes combine with lysosomes, allowing proteases to reach the endosome. As a result, peak intensities increase responding with protein structures on the other hand peak intensities reduction responding to phospholipid structures may suggest endosome motion from early endosomes to lysosomes.

The intensities of 650 cm^{-1} -C-C twisting of Tyr-, 750 cm^{-1} -Symmetric breathing of tryptophan-,880 cm^{-1} –Tryptophan-, 1000 cm^{-1} –phenylalanine-, 1215 cm^{-1} –Protein- relatively changed. Purine deprivation appears as 6-MP blocks the novo purine synthesis lead to induction of DNA synthesis, cell proliferation reduction also cytotoxicity [205]. Along with in vitro trials shown which de novo purine synthesis inhibition by 6-MP demonstrated cytotoxic effects [205,206] and in vivo [207,208] a necessary cofactor for activation of 6-MP [209]. This spectral changes corresponding to the protein upregulation structure in the endosomes. Further nucleotides spectral changes may related the energy production in endosomal acidification [210]. According to the t-test results, the C-C twisting of Tyr, tryptophan, phenylalanine, protein, lipid/collagen peaks changed significantly.

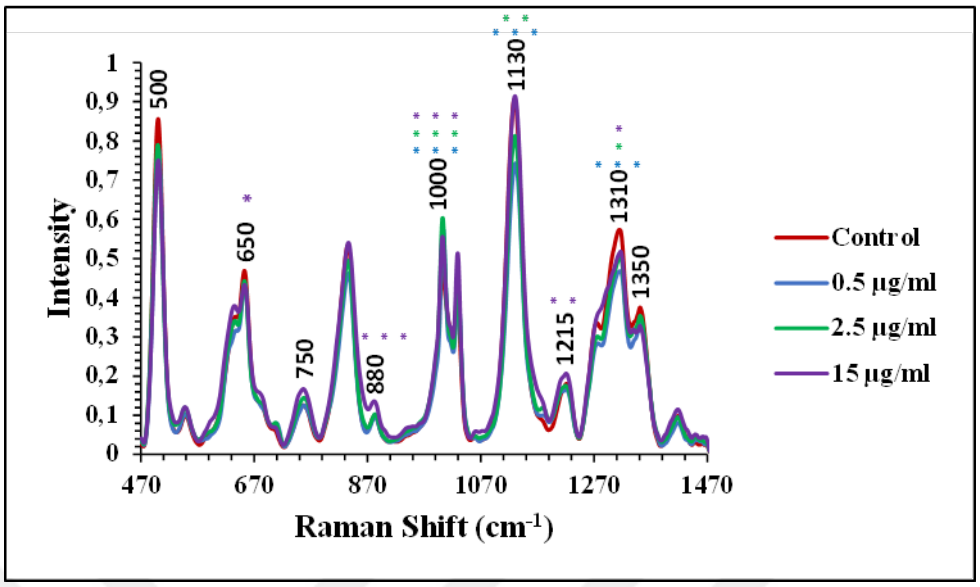

Figure 4.3.7. SERS spectra of A549 cell line at increasing 6-MP concentrations (* for p≤0.05, ** for p≤0.01, ***for p≤0.001, *: represent to 0.5 µg/ml, *: represent to 2.5 µg/ml, *: represent to 15 µg/ml)

Figure 4.3.8. represents comparison of the major variations of first and second PCs of control or 6-MP treated A549 cells. The PC1 scores of control and 6-MP treated A549 cells was demonstrated in Figure 4.3.8. (a) The primary differences were detected after 6-MP treatment with positive contribution peak at 500 cm^{-1}, 650 cm^{-1}, 830 cm^{-1}, 1130 cm^{-1},1300 cm^{-1} contributed respectively, ν(S-S) gauche-gauche-gauche, Tyr, nucleic acids, phospholipid structural changes and lipids while negative contributions were observed from the peaks at 712 cm^{-1}, 880 cm^{-1}, 1000 cm^{-1},1030 cm^{-1}, 1230 cm^{-1}, 1430 cm^{-1} and 1460 cm^{-1} related to adenine, tryptophan, phenylalanine, phenylalanine of collagen, amide III, deoxyribose and lipids and collagen respectively. Figure 4.3.8. (b) Shows the PC2 scores of control and 6-MP treated A549 cells. The main difference in peak were observed at 510 cm^{-1}, 760 cm^{-1}, 844 cm^{-1}, 1194 cm^{-1}, 1300 cm^{-1}, 1350 cm^{-1} which are related to cysteine, pyrimidine ring breathing mode, polysaccharide structure, nucleic acids, lipids and guanine respectively. These changes on PC1 and PC2 are related to 6-MP mechanisms. 6-MP have effect on pathway of inhibition of *de novo* purine synthesis. Thus, nucleic acid also DNA/RNA components in cells changed. Morphological changes in apoptotic cell death are characterized by bleeping of the plasma membrane, nuclear fragmentation, chromatin

condensation, and apoptotic body creation also phospholipid degradation in the endolysosomal membrane structure [191, 211, 212].

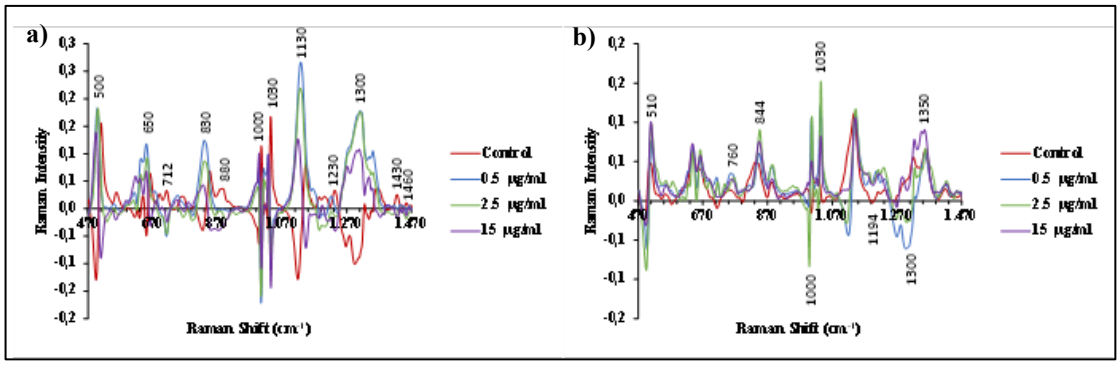

Figure 4.3.8. Comparison of (a) first and (b) second PCs of control and 6-MP treated A549cells

5. CONCLUSION AND FUTURE PERSPECTIVES

SERS is a powerful technique to analyze single-cells absence of labeling. SERS has been used for chemistry, physics, nanoscience and biological science, DNA hybridization, in vivo tumor targeting, biomolecules analysis including drug studies. In this study, it was shown that a label free SERS based approach to analysis of different drugs molecular mechanisms is illustrated. Thus, effects of drugs on normal and cancer cells were observed and it was found that SERS could be used to study the drug molecular mechanisms on single cells using the AuNPs as substrates.

The experimental design of SERS based system is quite easy. First, AuNPs with 50 nm average size were synthesized with a well-known citrate reduction. Then, beas-2b and A549 cells were exposed to a volume of colloidal suspension of 50 nm AuNPs. After 24-hour AuNPs incubation, the cells were exposed to Metformin and 6-Mercaptopurine for 24 hours. Finally, single cell analysis was achieved by mapping an area of living single cell and the collected spectra were analyzed. An attempt to relate the spectral changes to the metabolic changes were made.

The interpretation of spectral information from the Metformin treated cells is made in the light of the molecular pathways of the drug. In Beas-2b cells, the intensities attributed to PO_2^- stretch of nucleic acids, cytosine/guanine, cellular nucleic acids, and/or guanine 830 cm^{-1}, 1180 cm^{-1}, 1222 cm^{-1}, and 1350 cm^{-1}, respectively, are changed after the MET treatment, respectively. These intensity changes are attributed to increased AMPK activation through MET treatment. In addition, mTOR1 inhibitions cause cell proliferation and protein synthesis inhibition. Further, Metformin cause lipid inhibition. Therefore, the intensity changes at 1130 cm^{-1}, 1270 cm^{-1} and 1310 cm^{-1} attributed to variation in phospholipid composition.

The SERS spectra of Metformin exposed A549 cells shows some significant changes. The intensities of 592 cm^{-1} and 708 cm^{-1} peaks increase, and these peaks are attributed to glycerol and membrane phospholipids, respectively. Perhaps, this can be explained with the suppression of lipid and cholesterol biosynthesis. MET suppress lipid and cholesterol biosynthesis. These suppression mechanisms partially relevant to mitochondrial respiratory chain complex I as a temporary inhibition and also dependent on indirect AMPK activation.

The peaks at 635 cm^{-1}, 1030 cm^{-1}, 1000 cm^{-1}, 667 cm^{-1}, 830 cm^{-1}, 1222 cm^{-1}, 1350 cm^{-1} are attributed to methionine, phenylalanine of collagen, phenylalanine, T, G (DNA/RNA), nucleic acids, cellular nucleic acids, guanine peaks were changed, respectively. The peak at 926 cm^{-1} are attributed to proline and/or valine. The cause of inhibition of cell proliferation and protein synthesis AMPK activation mediated by mTORC1 signaling inhibition. Also, mTOR promotes nucleotides synthesis and cell growth via suppression of protein catabolism. It is thought that these metabolic changes of metformin cause the changes in the intensity of protein and nucleic acids peaks. Metformin may have a number of positive effects on the cell via modifying the endosomal compartments pH as well as lysosomes also late endosome. Metformin can influence cell metabolism via affecting endocytic cycle rate for receptor and transporter trafficking and autophagy, as well as directed activation or suppression of AMPK and/or mTOR by flipped the late endosome/lysosome states.

In addition, 6-Mercaptopurine molecular mechanisms was investigated by SERS. 6-Mercaptopurine effects on Beas-2b cells and it is that on guanine and DNA at 1350 cm^{-1} and 685 cm^{-1}. The reason for these effects that inhibition of *de novo* purine synthesis through 6-Mercaptopurine. Further, tyrosine and phenylalanine were change at 835 cm^{-1} and 1175 cm^{-1}. When the nucleic acids or DNA inhibits because the MET mechanisms, central dogma of gene expression that include replication transcription and translation pathways is inhibited. These mechanisms result inhibition of protein synthesis.

The intensities change of A549 cells which are treated with 6-Mercaptopurine were observed. Phospholipid structural changes, lipid/collagen, guanine peak intensities were changed at 1130 cm^{-1}, 1310 cm^{-1} and1350 cm^{-1}. This intensity changes might be due to initiation of apoptotic cell death mechanisms of 6-Mercaptopurine. Another aspect of those changes is that there are lipids in the endosomal membrane that are associated with the endosomal membrane identity. Both of these spectrum changes indicate that AuNPs' interaction with endosomal membrane decreased when early endosomes matured to late endosomes. The observed spectrum changes were dominated by biochemical changes in endosomal vesicles. Tyr, phenylalanine, protein and tryptophan peak intensities also change, respectively 650 cm^{-1}, 1000 cm^{-1}, 1215 cm^{-1} and 750/880 cm^{-1}. 6-Mercaptopurine cause de novo purine synthesis inhibitions this inhibition results with purine deprivation. Thus, cause DNA synthesis inhibitions, cell proliferation reduces and cytotoxicity. These results were observed possibly due to mechanism of the 6-Mercaptopurine. This might be due to the

initiation of 6-MP processes of apoptotic cell death pathways. Phosphatidylserine (PS) localization at the cell membrane's external surface, permeabilization of the mitochondrial membrane, cytochrome-c release, caspase activation, and breakage of inter-nucleosomal DNA are all well-known biochemical changes in apoptosis.

In conclusion, this study shows that the SERS could provide valuable molecular insight for the molecular effect of MET and 6-MP on the metabolic pathways. In this proof-of-concept study, it was found that SERS has the potential to monitor the cellular events in living cells. In order to understand the full potential of the technique for such studies, more comprehensive studies involving several cell lines and molecular techniques to verify the findings of the technique. Since the experimental conditions to obtain meaningful SERS data to correlate with the cellular responses is now established as demonstrated in this thesis, the very best future step is going to test the technique through well know cellular pathways to full clarification of the technique.

REFERENCES

[1] Raman C V., Krishnan KS. A new type of secondary radiation [11]. *Nature*. Epub ahead of print 1928. DOI: 10.1038/121501c0.

[2] Lohumi S, Kim MS, Qin J, et al. Raman imaging from microscopy to macroscopy: Quality and safety control of biological materials. *TrAC - Trends in Analytical Chemistry* 2017; 93: 183–98.

[3] Smith R, Wright KL, Ashton L. Raman spectroscopy: An evolving technique for live cell studies. *Analyst* 2016; 141: 3590–600.

[4] Uzunbajakava N, Lenferink A, Kraan Y, et al. Nonresonant confocal Raman imaging of DNA and protein distribution in apoptotic cells. *Biophys J* 2003; 84: 3968–81.

[5] Uzunbajakava N, Lenferink A, Kraan Y, et al. Nonresonant Raman imaging of protein distribution in single human cells. *Biopolym - Biospectroscopy Sect* 2003; 72: 1–9.

[6] Van Manen HJ, Kraan YM, Roos D, et al. Single-cell Raman and fluorescence microscopy reveal the association of lipid bodies with phagosomes in leukocytes. *Proc Natl Acad Sci U S A* 2005; 102: 10159–64.

[7] Matthäus C, Boydston-White S, Miljković M, et al. Raman and infrared microspectral imaging of mitotic cells. *Appl Spectrosc* 2006; 60: 1–8.

[8] Krafft C, Knetschke T, Funk RHW, et al. Studies on stress-induced changes at the subcellular level by Raman microspectroscopic mapping. *Anal Chem* 2006; 78: 4424–29.

[9] Chan JW, Taylor DS, Thompson DL. The effect of cell fixation on the discrimination of normal and leukemia cells with laser tweezers Raman spectroscopy. *Biopolymers* 2009; 91: 132–39.

[10] Kuzmin AN, Pliss A, Prasad PN. Changes in biomolecular profile in a single nucleolus during cell fixation. *Anal Chem* 2014; 86: 10909–16.

[11] Draux F, Gobinet C, Sulé-Suso J, et al. Raman spectral imaging of single cancer

cells: Probing the impact of sample fixation methods. In: *Analytical and Bioanalytical Chemistry*. 2010, pp. 2727–37.

[12] Meade AD, Clarke C, Draux F, et al. Studies of chemical fixation effects in human cell lines using Raman microspectroscopy. *Anal Bioanal Chem* 2010; 396: 1781–91.

[13] Wood BR, Hammer L, Davis L, et al. Raman microspectroscopy and imaging provides insights into heme aggregation and denaturation within human erythrocytes. *J Biomed Opt* 2005; 10: 014005.

[14] Moradi H, Ahmad A, Shepherdson D, et al. Raman micro-spectroscopy applied to treatment resistant and sensitive human ovarian cancer cells. *J Biophotonics* 2017; 10: 1327–34.

[15] Corsetti S, Rabl T, McGloin D, et al. Raman spectroscopy for accurately characterizing biomolecular changes in androgen-independent prostate cancer cells. *J Biophotonics*; 11. Epub ahead of print 2018. DOI: 10.1002/jbio.201700166.

[16] Matthews Q, Jirasek A, Lum JJ, et al. Biochemical signatures of in vitro radiation response in human lung, breast and prostate tumour cells observed with Raman spectroscopy. *Phys Med Biol*. Epub ahead of print 2011. DOI: 10.1088/0031-9155/56/21/006.

[17] Marro M, Nieva C, De Juan A, et al. Unravelling the Metabolic Progression of Breast Cancer Cells to Bone Metastasis by Coupling Raman Spectroscopy and a Novel Use of Mcr-Als Algorithm. *Anal Chem* 2018; 90: 5594–602.

[18] Bi X, Rexer B, Arteaga CL, et al. Evaluating HER2 amplification status and acquired drug resistance in breast cancer cells using Raman spectroscopy. *J Biomed Opt* 2014; 19: 025001.

[19] Swain RJ, Jell G, Stevens MM. Non-invasive analysis of cell cycle dynamics in single living cells with Raman micro-spectroscopy. *J Cell Biochem* 2008; 104: 1427–38.

[20] Notingher I, Jell G, Lohbauer U, et al. In situ non-invasive spectral discrimination between bone cell phenotypes used in tissue engineering. *J Cell Biochem* 2004; 92: 1180–92.

[21] Krishna CM, Sockalingum GD, Kegelaer G, et al. Micro-Raman spectroscopy of mixed cancer cell populations. In: *Vibrational Spectroscopy*. 2005, pp. 95–100.

[22] Schie IW, Huser T. Methods and applications of Raman microspectroscopy to single-cell analysis. In: *Applied Spectroscopy*. 2013, pp. 813–28.

[23] Nawaz H, Bonnier F, Knief P, et al. Evaluation of the potential of Raman microspectroscopy for prediction of chemotherapeutic response to cisplatin in lung adenocarcinoma. In: *Analyst*. 2010. Epub ahead of print 2010. DOI: 10.1039/c0an00541j.

[24] Draux F, Gobinet C, Sulé-Suso J, et al. Raman imaging of single living cells: Probing effects of non-cytotoxic doses of an anti-cancer drug. *Analyst*. Epub ahead of print 2011. DOI: 10.1039/c0an00998a.

[25] Yao H, Tao Z, Ai M, et al. Raman spectroscopic analysis of apoptosis of single human gastric cancer cells. *Vib Spectrosc* 2009; 50: 193–97.

[26] Dharani S, Rahman Z, Barakh Ali SF, et al. Quantitative estimation of phenytoin sodium disproportionation in the formulations using vibration spectroscopies and multivariate methodologies. *Int J Pharm* 2018; 539: 65–74.

[27] Yu LX, Amidon G, Khan MA, et al. Understanding pharmaceutical quality by design. *AAPS Journal* 2014; 16: 771–83.

[28] Salehi H, Middendorp E, Panayotov I, et al. Confocal Raman data analysis enables identifying apoptosis of MCF-7 cells caused by anticancer drug paclitaxel. *J Biomed Opt*. Epub ahead of print 2013. DOI: 10.1117/1.jbo.18.5.056010.

[29] Farhane Z, Bonnier F, Maher MA, et al. Differentiating responses of lung cancer cell lines to Doxorubicin exposure: in vitro Raman micro spectroscopy, oxidative stress and bcl-2 protein expression. *J Biophotonics*. Epub ahead of print 2017. DOI: 10.1002/jbio.201600019.

[30] Farhane Z, Nawaz H, Bonnier F, et al. In vitro label-free screening of chemotherapeutic drugs using Raman microspectroscopy: Towards a new paradigm of spectralomics. *Journal of Biophotonics*; 11. Epub ahead of print 2018. DOI: 10.1002/jbio.201700258.

[31] Fleischmann M, Hendra PJ, McQuillan AJ. Raman spectra of pyridine adsorbed at a silver electrode. *Chem Phys Lett* 1974; 26: 163–66.

[32] Jeanmaire DL, Van Duyne RP. Surface raman spectroelectrochemistry. Part I. Heterocyclic, aromatic, and aliphatic amines adsorbed on the anodized silver electrode. *J Electroanal Chem* 1977; 84: 1–20.

[33] Seki H. Raman spectra of molecules considered to be surface enhanced. *Stud Surf Sci Catal* 1986; 26: 289–310.

[34] Kneipp K, Kneipp H, Itzkan I, et al. Ultrasensitive Chemical Analysis by Raman Spectroscopy. *Chem Rev* 1999; 99: 2957–75.

[35] Guo H, He L, Xing B. Applications of surface-enhanced Raman spectroscopy in the analysis of nanoparticles in the environment. *Environmental Science: Nano* 2017; 4: 2093–107.

[36] Schatz GC. Theoretical Studies of Surface Enhanced Raman Scattering. *Acc Chem Res* 1984; 17: 370–76.

[37] Saleh TA. Pharmaceutical Characterization and Detection Using Surface-Enhanced Raman Scattering. *Int Arch Clin Pharmacol*. Epub ahead of print 2017. DOI: 10.23937/2572-3987.1510010.

[38] Nabiev IR, Morjani H, Manfait M. Selective analysis of antitumor drug interaction with living cancer cells as probed by surface-enhanced Raman spectroscopy. *Eur Biophys J* 1991; 19: 311–16.

[39] Kneipp K, Haka AS, Kneipp H, et al. Surface-enhanced raman spectroscopy in single living cells using gold nanoparticles. *Appl Spectrosc*. Epub ahead of print 2002. DOI: 10.1366/0003702021954557.

[40] Altunbek M, Kuku G, Culha M. Gold nanoparticles in single-cell analysis for surface enhanced Raman scattering. *Molecules*; 21. Epub ahead of print 2016. DOI: 10.3390/molecules21121617.

[41] Eliasson C, Lorén A, Engelbrektsson J, et al. Surface-enhanced Raman scattering imaging of single living lymphocytes with multivariate evaluation. *Spectrochim Acta - Part A Mol Biomol Spectrosc* 2005; 61: 755–60.

[42] Huang X, El-Sayed IH, Qian W, et al. Cancer cells assemble and align gold nanorods conjugated to antibodies to produce highly enhanced, sharp, and polarized surface Raman spectra: A potential cancer diagnostic marker. *Nano Lett*. Epub ahead of print 2007. DOI: 10.1021/nl070472c.

[43] Shamsaie A, Heim J, Yanik AA, et al. Intracellular quantification by surface enhanced Raman spectroscopy. *Chem Phys Lett* 2008; 461: 131–35.

[44] Fujita K, Ishitobi S, Hamada K, et al. Time-resolved observation of surface-enhanced Raman scattering from gold nanoparticles during transport through a living cell. *J Biomed Opt*. Epub ahead of print 2009. DOI: 10.1117/1.3119242.

[45] *Surface-Enhanced Raman Scattering – Physics and Applications*. 2006. Epub ahead of print 2006. DOI: 10.1007/11663898.

[46] Schlücker S. *Surface Enhanced Raman Spectroscopy: Analytical, Biophysical and Life Science Applications*. 2010. Epub ahead of print 2010. DOI: 10.1002/9783527632756.

[47] Hossain MK, Kitahama Y, Huang GG, et al. Surface-enhanced raman scattering: Realization of localized surface plasmon resonance using unique substrates and methods. *Analytical and Bioanalytical Chemistry* 2009; 394: 1747–60.

[48] Kitahama Y, Hossain MK, Ozaki Y, et al. Surface-Enhanced Raman Scattering Imaging: Application and Experimental Approach by Far-Field with Conventional Setup. In: *Raman, Infrared, and Near-Infrared Chemical Imaging*. 2011. Epub ahead of print 2011. DOI: 10.1002/9780470768150.ch15.

[49] Barhoumi A, Halas NJ. Label-free detection of DNA hybridization using surface enhanced Raman spectroscopy. *J Am Chem Soc* 2010; 132: 12792–93.

[50] Qian X, Peng XH, Ansari DO, et al. In vivo tumor targeting and spectroscopic detection with surface-enhanced Raman nanoparticle tags. *Nat Biotechnol* 2008; 26: 83–90.

[51] Han XX, Ozaki Y, Zhao B. Label-free detection in biological applications of surface-enhanced Raman scattering. *TrAC - Trends in Analytical Chemistry* 2012; 38: 67–78.

[52] Tang HW, Yang XB, Kirkham J, et al. Probing intrinsic and extrinsic components in single osteosarcoma cells by near-infrared surface-enhanced Raman scattering. *Anal Chem* 2007; 79: 3645–53.

[53] Aioub M, El-Sayed MA. A Real-Time Surface Enhanced Raman Spectroscopy Study of Plasmonic Photothermal Cell Death Using Targeted Gold Nanoparticles. *J Am Chem Soc*. Epub ahead of print 2016. DOI: 10.1021/jacs.5b10997.

[54] Litti L, Ramundo A, Biscaglia F, et al. A surface enhanced Raman scattering based colloid nanosensor for developing therapeutic drug monitoring. *J Colloid Interface Sci*. Epub ahead of print 2019. DOI: 10.1016/j.jcis.2018.08.107.

[55] Han G, Liu R, Han MY, et al. Label-free surface-enhanced raman scattering imaging to monitor the metabolism of antitumor drug 6-mercaptopurine in living cells. *Anal Chem*. Epub ahead of print 2014. DOI: 10.1021/ac503539w.

[56] Yang J, Cui Y, Zong S, et al. Tracking multiplex drugs and their dynamics in living cells using the label-free surface-enhanced raman scattering technique. *Mol Pharm*. Epub ahead of print 2012. DOI: 10.1021/mp200667d.

[57] Dowling RJO, Goodwin PJ, Stambolic V. Understanding the benefit of metformin use in cancer treatment. *BMC Medicine*; 9. Epub ahead of print 2011. DOI: 10.1186/1741-7015-9-33.

[58] Bailey CJ, Day C. Traditional plant medicines as treatments for diabetes. *Diabetes Care*; 12. Epub ahead of print 1989. DOI: 10.2337/diacare.12.8.553.

[59] Witters LA. The blooming of the French lilac. *Journal of Clinical Investigation*. Epub ahead of print 2001. DOI: 10.1172/JCI14178.

[60] Hesse E, Taubmann G. Die Wirkung des Biguanids und seiner Derivate auf den Zuckerstoffwechsel. *Arch für Exp Pathol und Pharmakologie* 1929; 142: 290–308.

[61] Adak T, Samadi A, Ünal AZ, et al. A reappraisal on metformin. *Regulatory Toxicology and Pharmacology* 2018; 92: 324–32.

[62] Fischer J, Ganellin CR. *Analogue-Based Drug Discovery II*. 2010. Epub ahead of print 2010. DOI: 10.1002/9783527630035.

[63] Thomas I, Gregg B. Metformin; a review of its history and future: from lilac to

longevity. *Pediatric Diabetes* 2017; 18: 10–16.

[64] Guariguata L, Whiting DR, Hambleton I, et al. Global estimates of diabetes prevalence for 2013 and projections for 2035. *Diabetes Res Clin Pract* 2014; 103: 137–49.

[65] Hundal RS, Krssak M, Dufour S, et al. Mechanism by which metformin reduces glucose production in type 2 diabetes. *Diabetes*. Epub ahead of print 2000. DOI: 10.2337/diabetes.49.12.2063.

[66] Mclntyre HD, Paterson CA, Ma A, et al. Metformin increases insulin sensitivity and basal glucose clearance in Type 2 (non-insulin dependent) diabetes mellitus. *Aust N Z J Med*. Epub ahead of print 1991. DOI: 10.1111/j.1445-5994.1991.tb01375.x.

[67] Fontaine E. Metformin-Induced Mitochondrial Complex I Inhibition: Facts, Uncertainties, and Consequences. *Front Endocrinol (Lausanne)*; 9. Epub ahead of print 2018. DOI: 10.3389/fendo.2018.00753.

[68] Li Gonga, Srijib Goswamic, Kathleen M. Giacominic, Russ B. Altmana,b and TEK. Metformin pathways: pharmacokinetics and pharmacodynamics. *Pharmacogenet Genomics* 2012; 22: 820–27.

[69] Foretz M, Guigas B, Bertrand L, et al. Metformin: From mechanisms of action to therapies. *Cell Metabolism* 2014; 20: 953–66.

[70] OWEN MR, DORAN E, HALESTRAP AP. Evidence that metformin exerts its anti-diabetic effects through inhibition of complex 1 of the mitochondrial respiratory chain. *Biochem J* 2000; 348: 607–14.

[71] Viollet B, Guigas B, Sanz Garcia N, et al. Cellular and molecular mechanisms of metformin: An overview. *Clinical Science* 2012; 122: 253–70.

[72] El-Mir MY, Nogueira V, Fontaine E, et al. Dimethylbiguanide inhibits cell respiration via an indirect effect targeted on the respiratory chain complex I. *J Biol Chem* 2000; 275: 223–28.

[73] Stephenne X, Foretz M, Taleux N, et al. Metformin activates AMP-activated protein kinase in primary human hepatocytes by decreasing cellular energy status. *Diabetologia* 2011; 54: 3101–10.

[74] Repiščák P, Erhardt S, Rena G, et al. Biomolecular mode of action of metformin in relation to its copper binding properties. *Biochemistry* 2014; 53: 787–95.

[75] Logie L, Harthill J, Patel K, et al. Cellular responses to the metal-binding properties of metformin. *Diabetes* 2012; 61: 1423–33.

[76] Bridges HR, Jones AJY, Pollak MN, et al. Effects of metformin and other biguanides on oxidative phosphorylation in mitochondria. *Biochem J* 2014; 462: 475–87.

[77] Drahota Z, Palenickova E, Endlicher R, et al. Biguanides inhibit complex I, II and IV of rat liver mitochondria and modify their functional properties. *Physiol Res* 2014; 63: 1–11.

[78] Andrzejewski S, Siegel PM, St-Pierre J. Metabolic profiles associated with metformin efficacy in cancer. *Frontiers in Endocrinology*; 9. Epub ahead of print 2018. DOI: 10.3389/fendo.2018.00372.

[79] Carling D, Mayer F V., Sanders MJ, et al. AMP-activated protein kinase: Nature's energy sensor. *Nature Chemical Biology* 2011; 7: 512–18.

[80] Zhou G, Myers R, Li Y, et al. Role of AMP-activated protein kinase in mechanism of metformin action. *J Clin Invest* 2001; 108: 1167–74.

[81] Shaw RJ, Lamia KA, Vasquez D, et al. Medicine: The kinase LKB1 mediates glucose homeostasis in liver and therapeutic effects of metformin. *Science (80-)* 2005; 310: 1642–46.

[82] Correia S, Carvalho C, Santos M, et al. Mechanisms of Action of Metformin in Type 2 Diabetes and Associated Complications: An Overview. *Mini-Reviews Med Chem* 2008; 8: 1343–54.

[83] Pernicova I, Korbonits M. Metformin-Mode of action and clinical implications for diabetes and cancer. *Nature Reviews Endocrinology* 2014; 10: 143–56.

[84] Gunton JE, Delhanty PJD, Takahashi SI, et al. Metformin rapidly increases insulin receptor activation in human liver and signals preferentially through insulin-receptor substrate-2. *J Clin Endocrinol Metab* 2003; 88: 1323–32.

[85] Bailey CJ, Turner RC. Metformin. *New England Journal of Medicine*. Epub ahead

of print 1996. DOI: 10.5005/jp/books/11384_11.

[86] Miller RA, Chu Q, Xie J, et al. Biguanides suppress hepatic glucagon signalling by decreasing production of cyclic AMP. *Nature* 2013; 494: 256–60.

[87] Alengrin F, Grossi G, Canivet B, et al. Inhibitory effects of metformin on insulin and glucagon action in rat hepatocytes involve post-receptor alterations. *Diabete Metab* 1987; 13: 591–97.

[88] Consoli A, Nurjhan N. Contribution of gluconeogenesis to overall glucose output in diabetic and nondiabetic men. *Ann Med* 1990; 22: 191–95.

[89] Stumvoll M, Nurjhan N, Perriello G, et al. Metabolic Effects of Metformin in Non-Insulin-Dependent Diabetes Mellitus. *N Engl J Med* 1995; 333: 550–54.

[90] Lutz TA, Estermann A, Haag S, et al. Depolarization of the liver cell membrane by metformin. *Biochim Biophys Acta - Biomembr* 2001; 1513: 176–84.

[91] Otto M, Breinholt J, Westergaard N. Metformin inhibits glycogen synthesis and gluconeogenesis in cultured rat hepatocytes. *Diabetes, Obes Metab* 2003; 5: 189–94.

[92] Lin HZ, Yang SQ, Chuckaree C, et al. Metformin reverses fatty liver disease in obese, leptin-deficient mice. *Nat Med* 2000; 6: 998–1003.

[93] Woo SL, Xu H, Li H, et al. Metformin ameliorates hepatic steatosis and inflammation without altering adipose phenotype in diet-induced obesity. *PLoS One*. Epub ahead of print 2014. DOI: 10.1371/journal.pone.0091111.

[94] Marchesini G, Brizi M, Bianchi G, et al. Metformin in non-alcoholic steatohepatitis. *Lancet* 2001; 358: 893–94.

[95] Geerling JJ, Boon MR, Van Der Zon GC, et al. Metformin lowers plasma triglycerides by promoting vldl-triglyceride clearance by brown adipose tissue in mice. *Diabetes* 2014; 63: 880–91.

[96] Zang M, Zuccollo A, Hou X, et al. AMP-activated protein kinase is required for the lipid-lowering effect of metformin in insulin-resistant human HepG2 cells. *J Biol Chem* 2004; 279: 47898–905.

[97] Fullerton MD, Galic S, Marcinko K, et al. Single phosphorylation sites in Acc1 and

Acc2 regulate lipid homeostasis and the insulin-sensitizing effects of metformin. *Nat Med* 2013; 19: 1649–54.

[98] Crompton M. The mitochondrial permeabitity transition pore and its role in cell death. *Biochemical Journal* 1999; 341: 233–49.

[99] Fontaine E, Eriksson O, Ichas F, et al. Regulation of the permeability transition pore in skeletal muscle mitochondria modulation by electron flow through the respiratory chain complex I. *J Biol Chem* 1998; 273: 12662–68.

[100] Dumas JF, Argaud L, Cottet-Rousselle C, et al. Effect of transient and permanent permeability transition pore opening on NAD(P)H localization in intact cells. *J Biol Chem* 2009; 284: 15117–25.

[101] Kantrow SP, Piantadosi CA. Release of cytochrome C from liver mitochondria during permeability transition. *Biochem Biophys Res Commun* 1997; 232: 669–71.

[102] Detaille D, Guigas B, Chauvin C, et al. Metformin prevents high-glucose-induced endothelial cell death through a mitochondrial permeability transition-dependent process. *Diabetes* 2005; 54: 2179–87.

[103] Lablanche S, Cottet-Rousselle C, Lamarche F, et al. Protection of pancreatic INS-1 β-cells from glucose- and fructose-induced cell death by inhibiting mitochondrial permeability transition with cyclosporine A or metformin. *Cell Death Dis*; 2. Epub ahead of print 2011. DOI: 10.1038/cddis.2011.15.

[104] Li B, Chauvin C, De Paulis D, et al. Inhibition of complex i regulates the mitochondrial permeability transition through a phosphate-sensitive inhibitory site masked by cyclophilin D. *Biochim Biophys Acta - Bioenerg* 2012; 1817: 1628–34.

[105] Loubiere C, Clavel S, Gilleron J, et al. The energy disruptor metformin targets mitochondrial integrity via modification of calcium flux in cancer cells /631/67/2327 /631/80 /13/106 /14/28 /96/95 /38/39 article. *Sci Rep*; 7. Epub ahead of print 2017. DOI: 10.1038/s41598-017-05052-2.

[106] Guigas B, Detaille D, Chauvin C, et al. Metformin inhibits mitochondrial permeability transition and cell death: A pharmacological in vitro study. *Biochem J* 2004; 382: 877–84.

[107] El-Mir MY, Detaille D, R-Villanueva G, et al. Neuroprotective role of antidiabetic drug metformin against apoptotic cell death in primary cortical neurons. *J Mol Neurosci* 2008; 34: 77–87.

[108] Lablanche S, Cottet-Rousselle C, Argaud L, et al. Respective effects of oxygen and energy substrate deprivation on beta cell viability. *Biochim Biophys Acta - Bioenerg* 2015; 1847: 629–39.

[109] Chen D, Xia D, Pan Z, et al. Metformin protects against apoptosis and senescence in nucleus pulposus cells and ameliorates disc degeneration in vivo. *Cell Death Dis*; 7. Epub ahead of print 2016. DOI: 10.1038/cddis.2016.334.

[110] Evans JMM, Donnelly LA, Emslie-Smith AM, et al. Metformin and reduced risk of cancer in diabetic patients. *Br Med J* 2005; 330: 1304–05.

[111] Bowker SL, Yasui Y, Veugelers P, et al. Glucose-lowering agents and cancer mortality rates in type 2 diabetes: Assessing effects of time-varying exposure. *Diabetologia* 2010; 53: 1631–37.

[112] Landman GWD, Kleefstra N, Van Hateren KJJ, et al. Metformin associated with lower cancer mortality in type 2 diabetes: Zodiac-16. *Diabetes Care* 2010; 33: 322–26.

[113] Bodmer M, Meier C, Krähenbühl S, et al. Long-term metformin use is associated with decreased risk of breast cancer. *Diabetes Care* 2010; 33: 1304–08.

[114] Wright JL, Stanford JL. Metformin use and prostate cancer in Caucasian men: Results from a population-based case-control study. *Cancer Causes Control* 2009; 20: 1617–22.

[115] Li D, Yeung SCJ, Hassan MM, et al. Antidiabetic Therapies Affect Risk of Pancreatic Cancer. *Gastroenterology* 2009; 137: 482–88.

[116] Sahra I Ben, Marchand-Brustel Y Le, Tanti JF, et al. Metformin in cancer therapy: A new perspective for an old antidiabetic drug? *Molecular Cancer Therapeutics* 2010; 9: 1092–99.

[117] Sachdev D, Yee D. Disrupting insulin-like growth factor signaling as a potential cancer therapy. *Molecular Cancer Therapeutics* 2007; 6: 1–12.

[118] Kalaany NY, Sabatini DM. Tumours with PI3K activation are resistant to dietary restriction. *Nature* 2009; 458: 725–31.

[119] Vander Heiden MG, Plas DR, Rathmell JC, et al. Growth Factors Can Influence Cell Growth and Survival through Effects on Glucose Metabolism. *Mol Cell Biol* 2001; 21: 5899–912.

[120] Morales DR, Morris AD. Metformin in cancer treatment and prevention. *Annu Rev Med* 2015; 66: 17–29.

[121] Shackelford DB, Abt E, Gerken L, et al. LKB1 Inactivation Dictates Therapeutic Response of Non-Small Cell Lung Cancer to the Metabolism Drug Phenformin. *Cancer Cell* 2013; 23: 143–58.

[122] Vazquez-Martin A, Colomer R, Brunet J, et al. Overexpression of fatty acid synthase gene activates HER1/HER2 tyrosine kinase receptors in human breast epithelial cells. *Cell Prolif* 2008; 41: 59–85.

[123] Ersoy C, Kiyici S, Budak F, et al. The effect of metformin treatment on VEGF and PAI-1 levels in obese type 2 diabetic patients. *Diabetes Res Clin Pract* 2008; 81: 56–60.

[124] Kalender A, Selvaraj A, Kim SY, et al. Metformin, independent of AMPK, inhibits mTORC1 in a rag GTPase-dependent manner. *Cell Metab* 2010; 11: 390–401.

[125] Sahra I Ben, Regazzetti C, Robert G, et al. Metformin, independent of AMPK, induces mTOR inhibition and cell-cycle arrest through REDD1. *Cancer Res* 2011; 71: 4366–72.

[126] Yu X, Mao W, Zhai Y, et al. Anti-tumor activity of metformin: From metabolic and epigenetic perspectives. *Oncotarget* 2017; 8: 5619–28.

[127] Gong J, Kelekar G, Shen J, et al. The expanding role of metformin in cancer: an update on antitumor mechanisms and clinical development. *Target Oncol* 2016; 11: 447–67.

[128] Leone A, Di Gennaro E, Bruzzese F, et al. New perspective for an old antidiabetic drug: Metformin as anticancer agent. *Cancer Treat Res* 2014; 159: 355–76.

[129] Eikawa S, Nishida M, Mizukami S, et al. Immune-mediated antitumor effect by type

2 diabetes drug, metformin. *Proc Natl Acad Sci U S A* 2015; 112: 1809–14.

[130] Prlic M, Williams MA, Bevan MJ. Requirements for CD8 T-cell priming, memory generation and maintenance. *Current Opinion in Immunology* 2007; 19: 315–19.

[131] Kim J, Lee HY, Ahn J, et al. NHX-5, Anl endosomal Na+/H+ exchanger, is associated with metformin action. *J Biol Chem* 2016; 291: 18591–99.

[132] Zhang CS, Li M, Ma T, et al. Metformin Activates AMPK through the Lysosomal Pathway. *Cell Metabolism* 2016; 24: 521–22.

[133] Kim J, You YJ. Regulation of organelle function by metformin. *IUBMB Life* 2017; 69: 459–69.

[134] Zhang CS, Jiang B, Li M, et al. The lysosomal v-ATPase-ragulator complex is a common activator for AMPK and mTORC1, acting as a switch between catabolism and anabolism. *Cell Metab* 2014; 20: 526–40.

[135] Fawal MA, Brandt M, Djouder N. MCRS1 binds and couples rheb to amino acid-dependent mTORC1 activation. *Dev Cell* 2015; 33: 67–81.

[136] Leto D, Saltiel AR. Regulation of glucose transport by insulin: Traffic control of GLUT4. *Nature Reviews Molecular Cell Biology* 2012; 13: 383–96.

[137] Kumar GP, Sanganal JS, Phani AR, et al. Anti-cancerous efficacy and pharmacokinetics of 6-mercaptopurine loaded chitosan nanoparticles. *Pharmacol Res* 2015; 100: 47–57.

[138] Wang CC, Chiou SS, Wu SM. Determination of mercaptopurine and its four metabolites by large-volume sample stacking with polarity switching in capillary electrophoresis. *Electrophoresis* 2005; 26: 2637–42.

[139] Kim JY, Ku YS. Enhanced absorption of indomethacin after oral or rectal administration of a self-emulsifying system containing indomethacin to rats. *Int J Pharm*. Epub ahead of print 2000. DOI: 10.1016/S0378-5173(99)00367-1.

[140] Podsiadlo P, Sinani VA, Bahng JH, et al. Gold nanoparticles enhance the anti-leukemia action of a 6-mercaptopurine chemotherapeutic agent. *Langmuir* 2008; 24: 568–74.

[141] Schwartz R, Stack J, Dameshek W. Effect of 6-Mercaptopurine on Antibody Production. *Proc Soc Exp Biol Med* 1958; 99: 164–67.

[142] Lennard L. The clinical pharmacology of 6-mercaptopurine. *Eur J Clin Pharmacol* 1992; 43: 329–39.

[143] Gearry RB, Barclay ML. Azathioprine and 6-mercaptopurine pharmacogenetics and metabolite monitoring in inflammatory bowel disease. *Journal of Gastroenterology and Hepatology (Australia)*. Epub ahead of print 2005. DOI: 10.1111/j.1440-1746.2005.03832.x.

[144] Cuffari C, Théorêt Y, Latour S, et al. 6-Mercaptopurine metabolism in Crohn's disease: Correlation with efficacy and toxicity. *Gut* 1996; 39: 401–06.

[145] Brogan M, Hiserodt J, Oliver M, et al. The effect of 6-mercaptopurine on natural killer-cell activities in Crohn's disease. *J Clin Immunol* 1985; 5: 204–11.

[146] Zimm S, Collins JM, Riccardi R, et al. Variable Bioavailability of Oral Mercaptopurine: Is Maintenance Chemotherapy in Acute Lymphoblastic Leukemia Being Optimally Delivered? *N Engl J Med*. Epub ahead of print 1983. DOI: 10.1056/NEJM198304283081705.

[147] Lennard L, Van Loon JA, Weinshilboum RM. Pharmacogenetics of acute azathioprine toxicity: Relationship to thiopurine methyltransferase genetic polymorphism. *Clin Pharmacol Ther* 1989; 46: 149–54.

[148] Su C, Lichtenstein GR. Treatment of inflammatory bowel disease with azathioprine and 6-mercaptopurine. *Gastroenterol Clin North Am* 2004; 33: 209–34.

[149] Tzoneva G, Dieck CL, Oshima K, et al. Clonal evolution mechanisms in NT5C2 mutant-relapsed acute lymphoblastic leukaemia. *Nature* 2018; 553: 511–14.

[150] Tiede I, Fritz G, Strand S, et al. CD28-dependent Rac1 activation is the molecular target of azathioprine in primary human CD4+ T lymphocytes. *J Clin Invest* 2003; 111: 1133–45.

[151] George P, Hernandez K, Hustu O, et al. A study of 'total therapy' of acute lymphocyticleukemia in children. *J Pediatr* 1968; 72: 399–408.

[152] Elion GB. The purine path to chemotherapy. *Science* 1989; 244: 41–47.

[153] Relling M V., Yanishevski Y, Nemec J, et al. Etoposide and antimetabolite pharmacology in patients who develop secondary acute myeloid leukemia. *Leukemia* 1998; 12: 346–52.

[154] Krynetskaia NF, Krynetski EY, Evans WE. Human RNase H-mediated RNA cleavage from DNA-RNA duplexes is inhibited by 6-deoxythioguanosine incorporation into DNA. *Mol Pharmacol*.

[155] LePage GA. Basic Biochemical Effects and Mechanism of Action of 6-Thioguanine. *Cancer Res* 1963; 23: 1202–06.

[156] Somerville L, Krynetski EY, Krynetskaia NF, et al. Structure and dynamics of thioguanine-modified duplex DNA. *J Biol Chem* 2003; 278: 1005–11.

[157] Iwaniec LM, Kroll JJ, Roethel WM, et al. Selective inhibition of sequence-specific protein-DNA interactions by incorporation of 6-thioguanine: Cleavage by restriction endonucleases. *Mol Pharmacol* 1991; 39: 299–306.

[158] Ceccotti S, Aquilina G, Macpherson P, et al. Processing of O6-methylguanine by mismatch correction in human cell extracts. *Curr Biol* 1996; 6: 1528–31.

[159] Durant ST, Morris MM, Illand M, et al. Dependence on RAD52 and RAD1 for anticancer drug resistance mediated by inactivation of mismatch repair genes. *Curr Biol* 1999; 9: 51–54.

[160] Morgan JA, Lynch J, Panetta JC, et al. Apoptosome activation, an important molecular instigator in 6-mercaptopurine induced Leydig cell death. *Sci Rep*; 5. Epub ahead of print 2015. DOI: 10.1038/srep16488.

[161] Kelley EE, Khoo NKH, Hundley NJ, et al. Hydrogen peroxide is the major oxidant product of xanthine oxidase. *Free Radic Biol Med* 2010; 48: 493–98.

[162] Bratton SB, Salvesen GS. Regulation of the Apaf-1-caspase-9 apoptosome. *Journal of Cell Science* 2010; 123: 3209–14.

[163] Allison AC. Immunosuppressive drugs: The first 50 years and a glance forward. *Immunopharmacology* 2000; 47: 63–83.

[164] Cara CJ, Pena AS, Sans M, et al. Reviewing the mechanism of action of thiopurine drugs: Towards a new paradigm in clinical practice. *Medical Science Monitor*; 10.

[165] Fernández-Ramos AA, Poindessous V, Marchetti-Laurent C, et al. The effect of immunosuppressive molecules on T-cell metabolic reprogramming. *Biochimie* 2016; 127: 23–36.

[166] Fernández-Ramos AA, Marchetti-Laurent C, Poindessous V, et al. 6-mercaptopurine promotes energetic failure in proliferating T cells. *Oncotarget* 2017; 8: 43048–60.

[167] Brands AJ. Applied Therapeutics - the Clinical Use of Drugs Fourth Edition. *Mil Med* 1990; 155: A18–A18.

[168] Gervasini G, Vagace JM. Impact of genetic polymorphisms on chemotherapy toxicity in childhood acute lymphoblastic leukemia. *Frontiers in Genetics*; 3. Epub ahead of print 2012. DOI: 10.3389/fgene.2012.00249.

[169] Weinshilboum RM, Sladek SL. Mercaptopurine pharmacogenetics: Monogenic inheritance of erythrocyte thiopurine methyltransferase activity. *Am J Hum Genet*.

[170] Lennard L, Lilleyman JS, Van Loon J, et al. Genetic variation in response to 6-mercaptopurine for childhood acute lymphoblastic leukaemia. *Lancet* 1990; 336: 225–29.

[171] Panetta JC, Evans WE, Cheok MH. Mechanistic mathematical modelling of mercaptopurine effects on cell cycle of human acute lymphoblastic leukaemia cells. *Br J Cancer* 2006; 94: 93–100.

[172] Kanemitsu H, Yamauchi H, Komatsu M, et al. 6-Mercaptopurine (6-MP) induces cell cycle arrest and apoptosis of neural progenitor cells in the developing fetal rat brain. *Neurotoxicol Teratol* 2009; 31: 104–09.

[173] Cheok MH, Evans WE. Acute lymphoblastic leukaemia: A model for the pharmacogenomics of cancer therapy. *Nature Reviews Cancer* 2006; 6: 117–29.

[174] Ehteshami M, Rasoulzadeh F, Mahboob S, et al. Characterization of 6-mercaptopurine binding to bovine serum albumin and its displacement from the binding sites by quercetin and rutin. *J Lumin* 2013; 135: 164–69.

[175] Karim H, Ghalali A, Lafolie P, et al. Differential role of thiopurine methyltransferase in the cytotoxic effects of 6-mercaptopurine and 6-thioguanine on human leukemia cells. *Biochem Biophys Res Commun* 2013; 437: 280–86.

[176] Gunnarsdottir S, Elfarra AA. Distinct tissue distribution of metabolites of the novel glutathione-activated thiopurine prodrugs cis-6-(2-acetylvlnylthio)purine and trans-6-(2-acetylvlnylthio)guaninee and 6-thioguanine in the mouse. *Drug Metab Dispos* 2003; 31: 718–26.

[177] Enüstün B V., Turkevich J. Coagulation of Colloidal Gold. *J Am Chem Soc* 1963; 85: 3317–28.

[178] Abdelhalim MAK, Mady MM, Ghannam MM. Physical properties of different gold nanoparticles: Ultraviolet-visible and fluorescence measurements. *J Nanomedicine Nanotechnol*; 3. Epub ahead of print 2012. DOI: 10.4172/2157-7439.1000133.

[179] Bailey CJ, Mynett KJ, Page T. Importance of the intestine as a site of metformin-stimulated glucose utilization. *Br J Pharmacol* 1994; 112: 671–75.

[180] Zhou G, Goodyear LJ, Moller DE, et al. Role of AMP-activated protein kinase in mechanism of metformin action Find the latest version : Role of AMP-activated protein kinase in mechanism of metformin action. *J Clin Invest*. Epub ahead of print 2001. DOI: 10.1172/JCI200113505.Introduction.

[181] Wang J, Gao Q, Wang D, et al. Metformin inhibits growth of lung adenocarcinoma cells by inducing apoptosis via the mitochondria-mediated pathway. *Oncol Lett* 2015; 10: 1343–49.

[182] Rena G, Hardie DG, Pearson ER. The mechanisms of action of metformin. *Diabetologia* 2017; 60: 1577–85.

[183] Madiraju AK, Erion DM, Rahimi Y, et al. Metformin suppresses gluconeogenesis by inhibiting mitochondrial glycerophosphate dehydrogenase. *Nature* 2014; 510: 542–46.

[184] DeCensi A, Puntoni M, Goodwin P, et al. Abstract PD03-03: Metformin and Cancer Risk in Diabetic Patients: A Systematic Review and Meta-Analysis, with Special Emphasis to Breast Cancer. 2010, pp. PD03-03-PD03-03.

[185] Kneipp J, Kneipp H, McLaughlin M, et al. In vivo molecular probing of cellular compartments with gold nanoparticles and nanoaggregates. *Nano Lett*. Epub ahead of print 2006. DOI: 10.1021/nl061517x.

[186] Scott CC, Vacca F, Gruenberg J. Endosome maturation, transport and functions. *Seminars in Cell and Developmental Biology* 2014; 31: 2–10.

[187] Yao J, Chen JM, Xu YB, et al. Enhancing the solubility of 6-mercaptopurine by formation of ionic cocrystal with zinc trifluoromethanesulfonate: Single-crystal-to-single-crystal transformation. *Cryst Growth Des* 2014; 14: 5019–25.

[188] Janjetovic K, Harhaji-Trajkovic L, Misirkic-Marjanovic M, et al. In vitro and in vivo anti-melanoma action of metformin. *Eur J Pharmacol* 2011; 668: 373–82.

[189] Cantrell LA, Zhou C, Mendivil A, et al. Metformin is a potent inhibitor of endometrial cancer cell proliferation-implications for a novel treatment strategy. *Gynecol Oncol* 2010; 116: 92–98.

[190] Kerr JFR, Wyllie AH, Currie AR. Apoptosis: A basic biological phenomenon with wide-ranging implications in tissue kinetics. *Br J Cancer* 1972; 26: 239–57.

[191] Elmore S. Apoptosis: A Review of Programmed Cell Death. *Toxicologic Pathology* 2007; 35: 495–516.

[192] Martina JA, Chen Y, Gucek M, et al. MTORC1 functions as a transcriptional regulator of autophagy by preventing nuclear transport of TFEB. *Autophagy* 2012; 8: 903–14.

[193] Rena G, Pearson ER, Sakamoto K. Molecular action and pharmacogenetics of metformin: current understanding of an old drug. *Diabetes Manag* 2012; 2: 439–52.

[194] Hardie DG, Carling D. The AMP-activated protein kinase. Fuel gauge of the mammalian cell? *European Journal of Biochemistry* 1997; 246: 259–73.

[195] Li P, Zhao M, Parris AB, et al. P53 is required for metformin-induced growth inhibition, senescence and apoptosis in breast cancer cells. *Biochem Biophys Res Commun* 2015; 464: 1267–74.

[196] Hsieh AC, Liu Y, Edlind MP, et al. The translational landscape of mTOR signalling steers cancer initiation and metastasis. *Nature* 2012; 485: 55–61.

[197] Porstmann T, Santos CR, Griffiths B, et al. SREBP Activity Is Regulated by mTORC1 and Contributes to Akt-Dependent Cell Growth. *Cell Metab* 2008; 8: 224–36.

[198] Ben-Sahra I, Hoxhaj G, Ricoult SJH, et al. mTORC1 induces purine synthesis through control of the mitochondrial tetrahydrofolate cycle. *Science (80-)* 2016; 351: 728–33.

[199] Feng Z, Hu W, De Stanchina E, et al. The regulation of AMPK β1, TSC2, and PTEN expression by p53: Stress, cell and tissue specificity, and the role of these gene products in modulating the IGF-1-AKT-mTOR pathways. *Cancer Res* 2007; 67: 3043–53.

[200] Saxton RA, Sabatini DM. mTOR Signaling in Growth, Metabolism, and Disease. *Cell* 2017; 168: 960–76.

[201] Settembre C, Zoncu R, Medina DL, et al. A lysosome-to-nucleus signalling mechanism senses and regulates the lysosome via mTOR and TFEB. *EMBO J* 2012; 31: 1095–108.

[202] Derijks LJJ, Gilissen LPL, Engels LGJB, et al. Pharmacokinetics of 6-mercaptopurine in patients with inflammatory bowel disease: Implications for therapy. *Ther Drug Monit*. Epub ahead of print 2004. DOI: 10.1097/00007691-200406000-00016.

[203] Dubinsky MC, Lamothe S, Yang HY, et al. Pharmacogenomics and metabolite measurement for 6-mercaptopurine therapy in inflammatory bowel disease. *Gastroenterology* 2000; 118: 705–13.

[204] Karran P, Attard N. Thiopurines in current medical practice: Molecular mechanisms and contributions to therapy-related cancer. *Nature Reviews Cancer* 2008; 8: 24–36.

[205] Bökkerink JPM, De Abreu RA, Bakker MAH, et al. Effects of methotrexate on purine and pyrimidine metabolism and cell-kinetic parameters in human malignant lymphoblasts of different lineages. *Biochem Pharmacol* 1988; 37: 2329–38.

[206] Dervieux T, Blanco JG, Krynetski EY, et al. Differing contribution of thiopurine methyltransferase to mercaptopurine versus thioguanine effects in human leukemic cells. *Cancer Res* 2001; 61: 5810–16.

[207] Bökkerink JPM, Bakker MAH, Hulscher TW, et al. Purine de novo synthesis as the basis of synergism of methotrexate and 6-mercaptopurine in human malignant

lymphoblasts of different lineages. *Biochem Pharmacol* 1988; 37: 2321–27.

[208] Bökkerink JPM, Bakker MAH, Hulscher TW, et al. Sequence-, time- and dose-dependent synergism of methotrexate and 6-mercaptopurine in malignant human T-lymphoblasts. *Biochem Pharmacol* 1986; 35: 3549–55.

[209] Dervieux T, Brenner TL, Hon YY, et al. De novo purine synthesis inhibition and antileukemic effects of mercaptopurine alone or in combination with methotrexate in vivo. *Blood* 2002; 100: 1240–47.

[210] Kneipp K, Kneipp H, Kneipp J. Surface-enhanced raman scattering in local optical fields of silver and gold nanoaggregates - From single-molecule raman spectroscopy to ultrasensitive probing in live cells. *Acc Chem Res* 2006; 39: 443–50.

[211] Häcker G. The morphology of apoptosis. *Cell and Tissue Research* 2000; 301: 5–17.

[212] Repnik U, Česen MH, Turk B. The endolysosomal system in cell death and survival. *Cold Spring Harb Perspect Biol*; 5. Epub ahead of print 2013. DOI: 10.1101/cshperspect.a008755.